Submicrometer-beam diffraction, fluorescence and absorption beamline in ALBA Synchrotron

Beamline construction Phase III

Gema Martínez-Criado
Andrés Cantarero
Mari-Cruz García-Gutiérrez
Fernando Garrido
Julio Pellicer-Porres
Adela Muñoz-Páez
Víctor López-Flores

With contributions from:
Laura Simonelli
Josep Nicolas

Submicrometer-beam diffraction, fluorescence and absorption beamline in ALBA Synchrotron

Beamline construction Phase III

Gema Martínez-Criado[1], Andrés Cantarero[2], Mari-Cruz García-Gutiérrez[3], Fernando Garrido[4], Julio Pellicer-Porres[5], Adela Muñoz-Páez[6], Víctor López-Flores[7]

With contributions from Laura Simonelli[8] and Josep Nicolas[8]

[1]European Synchrotron Radiation Facility, 38043 Grenoble Cedex, France.

[2]Institut de Ciència dels Materials, Universitat de València, 46980 Paterna (València), Spain

[3]Instituto de Estructura de la Materia (IEM-CSIC), Serrano 121, 28006 Madrid, Spain

[4]Museo Nacional de Ciencias Naturales (MNCN-CSIC), Calle Jose Gutierrez Abascal 2, 28006 Madrid, Spain

[5]Departamento de Física Aplicada-ICMUV, MALTA Consolider Team, Universitat de València, 46100 Burjassot (Valencia), Spain

[6]Departamento de Química Inorgánica, Facultad de Química, Universidad de Sevilla, 41012 Sevilla, Spain

[7]Synchrotron SOLEIL, L'Orme des Merisiers, St-Aubin, 91192, Gif-sur-Yvette, France

[8]CELLS - ALBA, Carretera BP 1413, 08290 Cerdanyola del Vallès, Barcelona, Spain

Summary

The Spanish and European user community face new scientific challenges in the study of hereterogeneous materials at micrometer and sub-micrometer scale. A synchrotron radiation beamline capable of performing micro X-ray diffraction and scattering (μ-XRD, to identify crystalline phases and μ-SAXS/WAXS, to detect long range order at the nm scale), micro X-ray fluorescence (μ-XRF, for chemical composition) and micro X-ray absorption (μ-XAS, to determine the local structure around selected elements) would be an invaluable tool to study these systems. On a second stage, it would also be desirable to be able to carry out fluorescence tomography, and holographic and/or ptychography imaging. The overall desired characteristics would be: sub-micron spatial resolution, sub-ppm detection limit, 2-20 keV energy range, and a versatile sample environment.

While the materials science and technology field, in particular the nanotechnology branch, seems to be the first beneficiary, the earth and environmental sciences, cultural heritage and bio-medicine fields will specially profit from this beamline, as heterogeneity and small size are inherent characteristics of their samples. This beamline will thus be a truly multidisciplinary instrument.

As a proof of the envisaged success of this beamline, similar versions of hard X-ray microprobe instruments already have a large and competitive established user base in the European scientific community. Within the Spanish community, more than twenty groups have already carried out experiments in this type of beamlines and many of them have already published the outcome of their works.

Table of Contents

Introduction

Over the last decade, the world-class performance of hard X-ray microprobes has led to many ground-breaking results in several areas such as environmental, earth and planetary science, cultural heritage, biomedical and materials sciences. Based on the great publication records and ever increasing user demand, a large number of third-generation microprobes are operating or are under construction, whilst several advanced projects are in the planning or development phase. Figure Error: Reference source not found indicates the X-ray microprobes currently operational at synchrotron radiation (SR) sources across the world and those planned or under construction. For example, the demands for beamtime in the last years at the ESRF have risen steadily to a level difficult to sustain that has indeed caused the construction of the new ID16A/B beamlines.

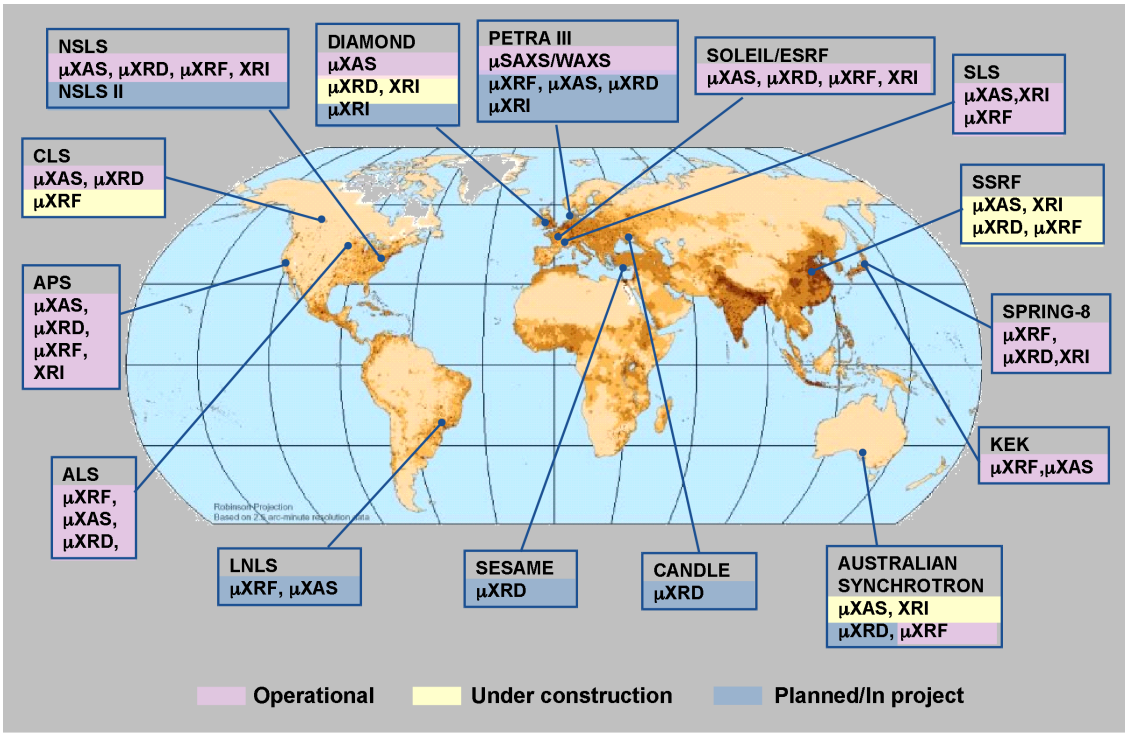

Figure 1: Existing and proposed microprobe and nanoprobe (in red) facilities in the world

However, there is still a critical need for significantly improve not only the microprobe availability but also its performance in terms of spatial resolution, beam stability, energy range, and detection schemes. Also the penetration power of hard X-rays could be used to extend the studies to specific sample environments at micrometer scales. Thus, the principal motivation of this beamline proposal is to respond to the Spanish user community which faces new scientific challenges in the study of hereterogeneous materials at micrometer scales, securing in the long term a forefront role of ALBA in SR based user science. Driven by those scientific inquiries and its large potential in Spain, the present document is designed to address both the quality and quantity of beamtime available based on the implementation of a

unique national research tool for a wide user community working on the above mentioned fields at ALBA. The interdisciplinarity among these scientific communities trigger several emerging and challenging projects with scientific target of high impacts in environment, health and social spheres. Current similar versions of hard X-ray microprobe instruments already have a large and competitive established user base in the European scientific community, who will also substantially benefit from it.

In general, synchrotron microprobes extend the capabilities of standard techniques, providing several benefits:

1. Capability to focus the SR to very small spot sizes while retaining high brightness that enables high spatial resolution and thus 'imaging' of elemental distribution and structure on a sub-micron scale.

2. Tunable beam excitation energy, which means that individual elements in the sample can be selected for analysis and imaging with total discrimination. For the special case of the beamline here proposed the energy range would be 2-20 keV, which covers the K absorption edges of elements from P upwards to Nb, and the L_3 edges from Y to U. This is particularly appropriate for the detection of trace elements in samples, and when coupled with the high brightness of the beam it is possible to analyse down to parts per billion level.

3. The element-specific character of XAS provides a useful complement to methods in which the entire sample matrix contributes to the signal, such as X-ray diffraction (XRD).

4. SR microprobes using undulator sources provide micron spatial resolution and sub-ppm detection limits for Z>20.

5. The ability to perform X-ray microdiffraction simultaneously with microfluorescence, allows determining mineralogy and crystal structure at the same time as one measures chemical composition and chemical state.

6. The possibility to record Small/Wide Angle X-ray Scattering measurements with the same setup and detector as the X-ray microdiffraction measurements.

7. The capability to work within in-situ in environmental chambers such as high or low temperature, high pressure or wet cells.

8. Capability to analyze buried objects such as fluid inclusions or micrometeorites embedded in aerogel.

The current and prospective needs in hard X-ray microanalysis of several scientific communities were expressed through discussions with project leaders in different scientific areas in a meeting organized in Barcelone in December 2008, and a first project was presented in the Phase II ALBA beamline construction in 2009. The proposal presented an outgrowth of these discussions though interactions with other scientific communities were also included. From this basis, the current proposal has an updated and more ambitious technical requirements in trend with the present technological advances, that has allowed a broader field of applicability, and thus an enlarged scientific case.

The document also highlights the wishes and needs for a combined use of the soft-X-ray microscopy, X-ray Absorption spectroscopy, and the foreseen hard- X-ray microprobe beamlines at ALBA for upscaling small scale information to large scale problems.

The project encompasses five major subjects well described below: 1. Earth and environmental sciences, 2. Cultural heritage, 3. Materials science: hard condensed matter, 4.

Materials science: soft condensed matter, and 5. Biomedical and bioenvironmental science. It foresees to deliver a new facility with unique associated environments for the scientific communities studying samples at sub-micrometer domains, providing unparalleled multilevel information necessary to answer a broad range of high impact questions. In Biology, for instance, the roles of trace metals in neurodegenerative diseases, or the bio-chemical tumor-related mechanisms at cellular levels in organisms can be searched. In Environmental and earth sciences it is important to know the driving phenomena behind pollution processes involving fly ashes and waste particles, or how the interiors of the Earth were formed, also the solubility of metals under hydrothermal conditions inside a diamond anvil cell. More oriented to materials sciences, some questions can be addressed, for instance can electro-migration be minimized in the manufacture of microelectronic devices? How can defect free lithographed-templates be fabricated? Therefore, the present proposal aims greatly extending the scientific impact of ALBA beyond that achievable within the current operation by the incorporation of a hard X-ray microprobe.

In addition, the μ-XRF-XRD-SAXS/WAXS-XAS combination has many applications to the manufacturing and engineering industries. Ageing of both plastics and alloys to form microcrystalline domains, sometimes accompanied by elemental diffusion, is an area that could benefit from this combination of analyses. Elemental partitioning is an area of particular importance to the microelectronics industry. The stresses resulting from corrosion, welding, annealing and ageing can be measured as a function of 3D on a micrometre scale using this methodology. This will enable not only a better understanding of component failure but through in situ process simulation can lead to design of materials with greater failure resistance.

The key objectives are twofold: first, the construction of a new station with a strong emphasis on the routine delivery of stable sub-microsized X-ray beams, and second, the development of simultaneous spectroscopic microanalysis and imaging by multimodal techniques in a broad energy range (2 - 20 keV) with the possibility of in-situ conditions.

Scientific cases

Earth and environmental sciences

Earth materials are often heterogeneous, so X-ray microbeam studies are valuable to unravelling this complexity. Most X-ray based methods can be applied with high spatial resolution, including X-ray fluorescence (XRF), X-ray diffraction (XRD), X-ray absorption fine structure (EXAFS and XANES) and computed microtomography (CMT). By applying these techniques in a nearly simultaneous fashion, it is possible to produce elemental maps with sub-part-per-million sensitivity and determine the speciation and mineralogy at selected localizations in the material. Toxic and radioactive elements are also amenable by this approach. Moreover, an additional advantage of using synchrotron light for investigating earth and environmental materials is the penetrating power of the radiation, which allows studies in conditions very close to the real ones, for example, in the presence of water.

A rapidly growing multidisciplinary field referred to as molecular environmental science has emerged during the last few years due to the unique role that synchrotron radiation sources have begun to play in addressing the above issues. The very high intensity, brightness, and energy tunability of X-rays from synchrotron storage rings has allowed element-specific spectroscopic studies of pollutants in highly complex environmental samples and at highly diluted levels. These type of studies have led to unique information on many of the chemical processes that affect contaminant elements at the solid-water interface, and they have provided a great deal of basic data on the speciation and spatial distribution of toxic species in environmental samples [Brown et al., 2002], The following are a few examples of X-ray microprobe analysis on this field.

Mineralogy, petrology and trace element geochemistry

Minerals are key components of rocks and provide unique information on their formation conditions. Their minor and trace element as well as isotope composition, provide important insights into the geochemical cycling of elements and can give us information about processes, origin and evolution of the Earth. By combining XAS and XRF, unique information on the location of trace elements in mineral structures is obtained, providing a crucial piece of information to understand the processes controlling mineral partitioning. This information is also important for understanding charge-compensation processes in minerals and for deriving realistic activity-composition relationship. The combination of μ-XRF, μ-XRD and μ-XAFS techniques is a powerful tool for this type of studies. This fact is clearly evidenced in the large number of scientific publications that include this methodology [Blundy and Wood, 2003].

Recent investigations have shown that red coralline algae record ambient temperature in their calcite skeletons. Temperature recorded by variation in Mg concentrations within algal growth bands has sub-annual resolution and high accuracy. The conversion of Mg concentration to temperature is based on the assumption that Ca is replaced by Mg within the algal calcite skeleton at high temperatures. While Mg-temperature relationships in coralline algae have been calibrated for some species, the location of Mg within the calcite lattice remains unknown. Critically, if Mg is not a lattice component but is associated with organic components this could lead to erroneous temperature records. Before coralline algae are used

in large scale climate reconstructions it is therefore important to determine the location of Mg. As shown in Figure 2 Mg-X-ray absorption near edge structure (XANES) indicates that Mg is associated with the calcite lattice in Lithothamnion glaciale and Phymatolithon calcareum coralline algae, where it is deposited in all seasons. These results suggest L. glaciale and P. calcareum are robust Mg-palaeotemperature proxies. It is suggested that similar confirmation be obtained for Mg associations in other species of red coralline algae aiding our understanding of their role in climate reconstruction at large spatial scales [Kamenos et al., 2009].

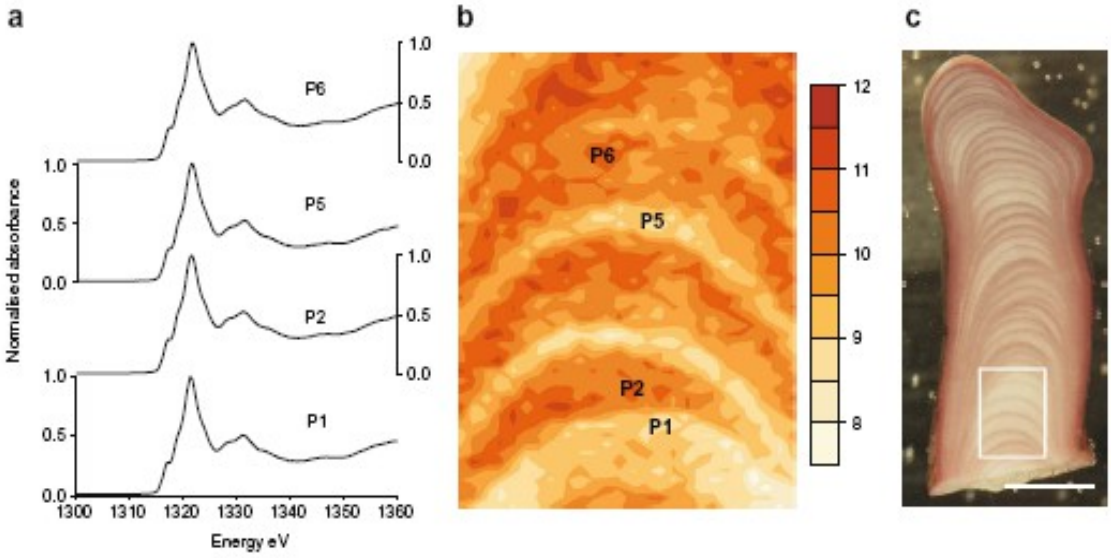

Figure 2: Mg XANES spectra of areas of summer (P2,P6) and winter (P1,P5) growth in contemporary free-living Lithothamnion glaciale (a) with associated Mg fluorescence contour map (b) and region of sample mapped/analysed (c). Scale bar = 1 mm. Scan resolution: 26X51 pixels

Interface and surface geochemistry

Another example of the usefulness of microprobe techniques applied on environmental problems is the identification of the site selectivity of metal adsorption in minerals which may be used in remediation processes. In Figure 3 the distributions of Co and U at a calcite (1014) surface is shown, revealing the correspondence of metal concentration with site distribution. The magnitude of differential uptake may exceed a factor of ten for some metals, which implies that differences in the availability of sites could change sorption characteristics of a mineral by a similar degree. A relevant finding of this work is that metals with similar size and charge may exhibit different preferences for sites. Other studies have shown that anions, including AsO_4^{3-}, SeO_4^{2-} and $UO_2(CO_3)_3^{4-}$ have distinct preferences for different surface sites indicating that the uptake of toxic species and radionuclides is controlled by the coordinative aspects of crystal surfaces. These data highlights the importance to the environmental scientists to include site preference information into their molecular models of contaminant uptake.

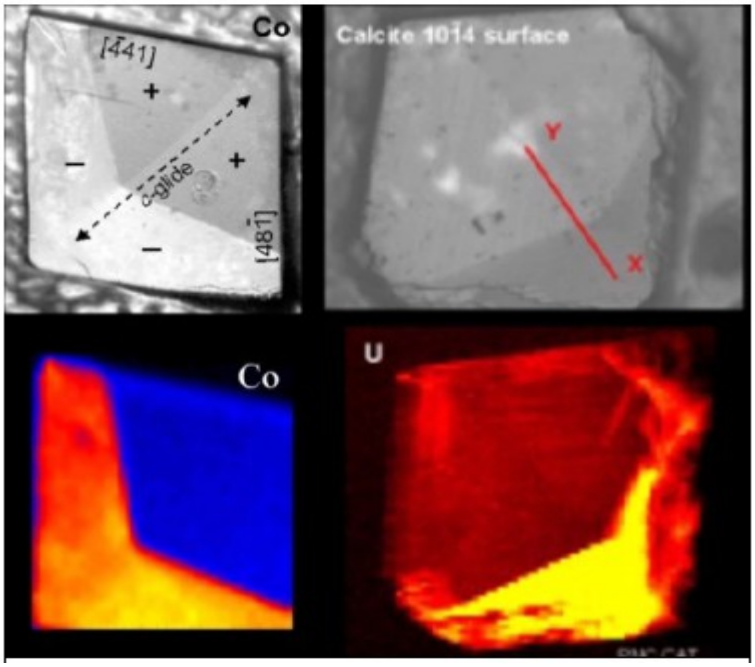

Figure 3: Differential-interference images (upper left and right) and μ-XRF images (lower left and right) of two calcite crystals showing the incorporation of cobalt and uranium (yellow = higher concentration). Reeder et al., 2001.

By using microfocused synchrotron-based XAS techniques, it is possible to determine the distribution and speciation of metals at the soil–water interface and in plant tissues, where speciation can vary over hundreds of microns. In addition being capable of examining the distribution and speciation of lighter elements has significantly enhanced our ability to probe elemental associations in natural systems [Parise and Brown, 2006]. In addition, XRF and synchrotron based μ-XRD methods are providing important insights into the formation and structure of nanominerals resulting from bacteriogenic processes. The study of mineral-bacteria interactions using synchrotron radiation methods is anticipated to grow significantly in coming years and to yield important new information on biomineralization, and the biogeochemical cycling of elements [Maurice and Hochella, 2008].

The formation of metallic copper nanoparticles at the soil-root interface has been studied by Manceau et al. (2008). The first commercial fungicide —the "Bordeaux mixture" of copper sulphate and lime— was used to fight downy mildew in French vineyards. The fungicide worked by catalyzing the production of free radicals that damage proteins and enzymes involved in cycling copper between Cu(I) and Cu(II) oxidation states in the cellular electron transport chain. However, not all fungi are sensitive to copper toxicity. Some, called mycorrhizae, which live underground in symbiosis with host plants through intracellular or extracellular colonization of their roots, are resistant, although the reason is unknown. Applying microfocus synchrotron techniques the authors has discovered a new form of copper —metallic nanoparticles—in the rhizosphere (soil-root interface) that may explain how mycorrhizal (symbiotic) fungi detoxify copper shown in Figure 4.

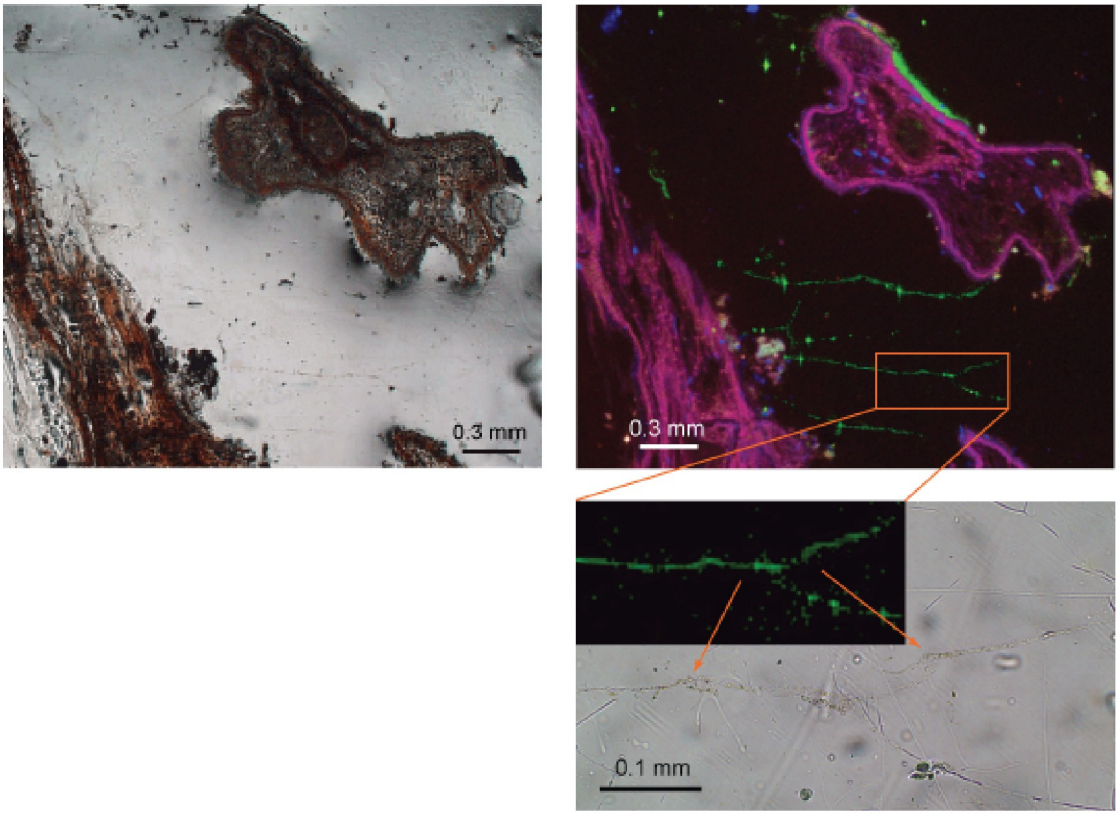

Figure 4: Left optical micrograph showing longitudinal (left) and transversal (right) sections of roots from Iris pseudoacorus. Top right micro x-ray fluorescence showing the distribution of zinc (red), copper (green), and calcium (blue). The longitudinal section (left) shows the association of nanoparticulate metallic copper with ramified (branched) mycorrhizal fungi; the transversal section (right) shows the association in a biofilm at the surface of the root. Bottom: enlargement of a ramified hypha (long, filamentous fungus cells). Resolution = 8 x 8 μm2.

The study of the chemical forms of Ni in tropical soils in the lateritic deposits from Moa Bay Cuba [Mosselmans et al. 2008] is another example of the use of μ-XRF and μ-XANES/EXAFS. These deposits are mainly classified as oxide-type and their profiles are generally constituted by essentially fine-grained minerals and precisely the small size of the mineral grains has distorted the knowledge of the crystallochemistry of the laterite-forming minerals. In Ni lateritic mineral deposits all the materials rich in Mn, Co and Ni are amorphous or of very low crystallinity, but the ore is also constituted by hematite, maghemite, goethite and lithiophorite and intermediate products. A detailed study to determine the mineral phases rich in Mn-Co-Ni has not been made for most lateritic deposits, while the oxidation state of Ni and the structural relationship of Ni with their bearing minerals is fully characterized. For this study a microfocused beam with a 5 micron spot size (the mineral grain size of 50-1000 microns) was used to map the sample for Mn, Fe and Ni. This allowed defining a region of interest and hot spots of Ni to be studied by means of μ-XANES/EXAFS. Ni speciation was investigated using μ-XANES and the local structure of Ni was determined by μ-EXAFS providing information on the distances and nature of the nearest neighboring atoms. The use of both μ-XRF and μ-XAS techniques helps gain some insights of Ni crystallochemistry in Moa Bay laterites and demonstrated that the Ni immobilized from the weathered basalts has been concentrated to Mn micronodules about 1 mm in diameter and probably adsorbed to the mineral surface.

Environmental geochemistry

Synchrotron microprobe techniques have been useful in the study of the chemical forms, the spatial distribution and the phase association of contaminants in mine wastes and soils contaminated by heavy metals, radionuclide, and they have been also used to the study of plants and fishes that hyper accumulate specific elements [Brown et al., 1999]. The study of soils, due to their importance and high reactivity that make them extremely sensitive to environmental modifications, had a great deal of attention and a great number of dedicated publications appeared focussed on the speciation of metallic pollutants being studied by means of X-ray absorption fine structure (EXAFS/XANES) spectroscopy. XAFS has revealed a well suited technique because of its element selectivity, sensitivity to the binding environment of the probed element, detection limit as low as about 100 mg/kg for most heavy metals and minimal sample preparation.

The most reactive sites in soils have particle sizes in the micrometer range, and metal speciation may vary over regions of a few 100 μm^2 making it difficult to ascertain the precise metal speciation with bulk XAFS. These include, for instance, colloids coming from soils and sediments, that have a an essential role on contamination transport.

However, state-of-the-art X-ray detectors and better beamline optics, produce microfocused beams for spectromicroscopy and imaging studies. These developments provide a means for probing element speciation and associations in heterogeneous materials such as soils and plants. Two examples from Spanish groups follow.

Mobility of As from mine wastes in natural systems

The prolonged mining activity in the Iberian Pyrite Belt (IBP), located in the southwest part of the Iberian Peninsula and dating back to pre-roman times, created one of the world's largest accumulations of mine wastes in which high concentrations of As have been detected. The fate and mobility of As in natural systems is controlled by attenuation through sorption and precipitation processes that are affected by geochemical properties of the system such as redox potential, pH and chemical composition. However, physical processes such as preferential flow (PF) through might have an effect on the speciation and distribution of As and therefore, might play an important role in contaminant mobility. The effect of this non-equilibrium physical phenomenon on As distribution and speciation in the river bank area of the São Domingos river downstream of the abandoned São Domingos Mine (South Portugal) is currently being analyzed. Chemical mapping using synchrotron μ-XRF and μ-XANES was performed on different samples from both matrix (MF) and preferential flow (PF) domains of the sediment profile. Data were collected at the SSRL with an X-ray beam focused to a 2 x 2 μm^2 spot size. Element maps were collected for As, Fe, Pb, Cu, Ca, K, Ti, Zn, Mn, Si, S, Cl and Cr using 5 μm step size. Arsenic μ-XANES spectra were collected on enriched As spots identified in the XRF maps and compared to background areas low in As and Fe.

Results indicated that As and Fe distributions were affected by preferential flow processes. Lower concentrations of both elements were observed in PF paths compared to the soil matrix. However, As speciation was not affected by this phenomenon as determined by XAS. Synchrotron μ-XRF mapping (~150 × 150 μm^2 areas) showed, in general, a high positive correlation between As and Fe (Figure). Moreover, similar As and Fe intensities were found in samples from both water flow domains. Analysis of arsenic μ-XANES indicated that As was present only as As(V). The As μ-XANES spectra of two spots analyzed in preferential flow domain could be fit a reference spectrum of As(V) sorbed on ferrihydrite (molar Fe/As=80). In samples from the matrix flow domain, two of the three As μ-XANES spectra

were fit with the same reference spectrum, however, in some spots As μ-XANES spectrum could be well fit with a mixture of 65% beudantite and 35% jarosite. While all the arsenic species identified in this study are stable under the acidic conditions found in this experimental site, As mobility is limited by sorption/trapping of As by amorphous iron oxides (e.g. ferrihydrite) which has a relatively long-term stabilization effect on contaminated sediments at low pH. Preferential flow phenomena might have an important effect on the stability of these trapping mineral phases [Helmhart, et al., 2014]

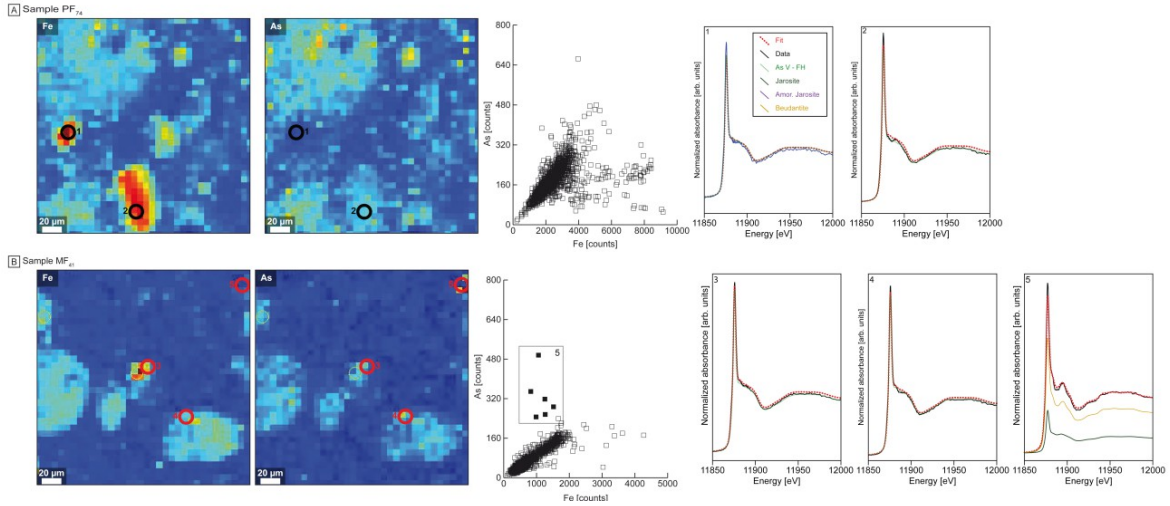

Figure 5: Synchrotron microfocused X-ray fluorescence (μ-XRF) As and Fe maps, As/Fe correlation plots and As μXANES plots of samples from matrix (MF) and preferential flow (PF) domains. Spots selected for μXANES are marked with a ring in the maps.

Toxic elements in colloids

Understanding the release of colloid particles from soils and sediments and their association with contaminants is essential to evaluate contaminant transport processes. Colloids are able to strongly bind metals. In soils and sediments impacted by mining waste, the mobility of As can be affected by the release and transport of colloids and nanoparticles from the soils. Samples were collected from an abandoned smelting factory located in Guadalix de la Sierra (Madrid, Spain). Arsenic-rich residues from metal ore smelting were dumped adjacent to the factory and pose a public health concern. The dispersable colloid fraction (DCF) (10nm-1000nm) of samples taken from the waste pile and adjacent sediments and soils were characterized physically, chemically and spectroscopically to assess colloid composition and natural partitioning of As between the dissolve and colloid fractions. We used Asymmetrical-Flow Field-Flow Fractionation (AsFlFFF) coupled to ICP-MS spectrometer to study element distribution as a function of particle size. Colloid samples were further characterized by transmission electron microscopy (TEM-EDX). X-ray absorption (XAS) spectroscopy was used to study As and Fe speciation in the colloid fraction. Chemical mapping using synchrotron microfocused X-ray fluorescence (XRF) was performed on the DCF samples. Synchrotron μ-XRF data were taken at the Stanford Synchrotron Radiation Lightsource (SSRL) at room temperature. X-ray energy was tuned to 12,500 eV and maps were collected in continuous raster scanning mode for As, Ca, Fe, Cu and Zn. Arsenic and Fe K-edge spectra of DCF samples, isolated on ultrafiltration membranes, were collected on bending-magnet

BM25A beamline (SpLine) at the European Synchrotron Radiation Facility (ESRF) at room temperature. Particulate scorodite (Ø~80nm) was observed by TEM-EDX in the waste colloid fraction (Fig. 6a). Imaging and analysis of the riverbed colloid fraction showed particle aggregates of <50 µm and high concentrations of Si, Al and Fe, which may suggest the presence of clay minerals and Fe hydroxides (Fig 6b). In the riverbed_2 sample, 30 nm Fe nanoparticles were identified with the presence of Si, Ca, Mn and Cu (Fig. 6c). TEM images showed that Fe nanoparticles form aggregates (Fig. 6d). Smaller Fe nanoparticles (10 nm) were observed in the subsoil colloid samples (Fig 6e) and formed larger aggregates (Ø~50nm). The colloid fraction of the sediment pond downstream contained aggregates of nanoparticles (Ø~10nm) and Fe, Si, Al, Ca, Mg and As were detected by EDX, indicating a heterogeneous aggregate. µ-XRF maps (1x 1µm^2) of elements in the sediment pond indicated correlation of As and Fe in aggregated nanoparticles (150-250nm) (Fig 6g and h). Our results indicates that Fe and Al are main components of the DCF of all the acidic downstream samples where As was found mainly retained on nanosize ferrihydrite. This association persists in the DCF of all the downstream samples regardless the specific geochemical characteristics of the samples. This indicates a high affinity of As for Fe-(oxy)hydroxides and a potential mobility of As bound to Fe nanoparticles. The combination of Asfl-FFF - ICP-Ms and micro X-ray absorption spectroscopy provides fundamental information of the partitioning of polluting elements in colloid-size particles as well as their molecular speciation in these particles, which is essential to evaluate the potential metal(oid) pollution processes in natural systems. [Serrano et al., 2014]

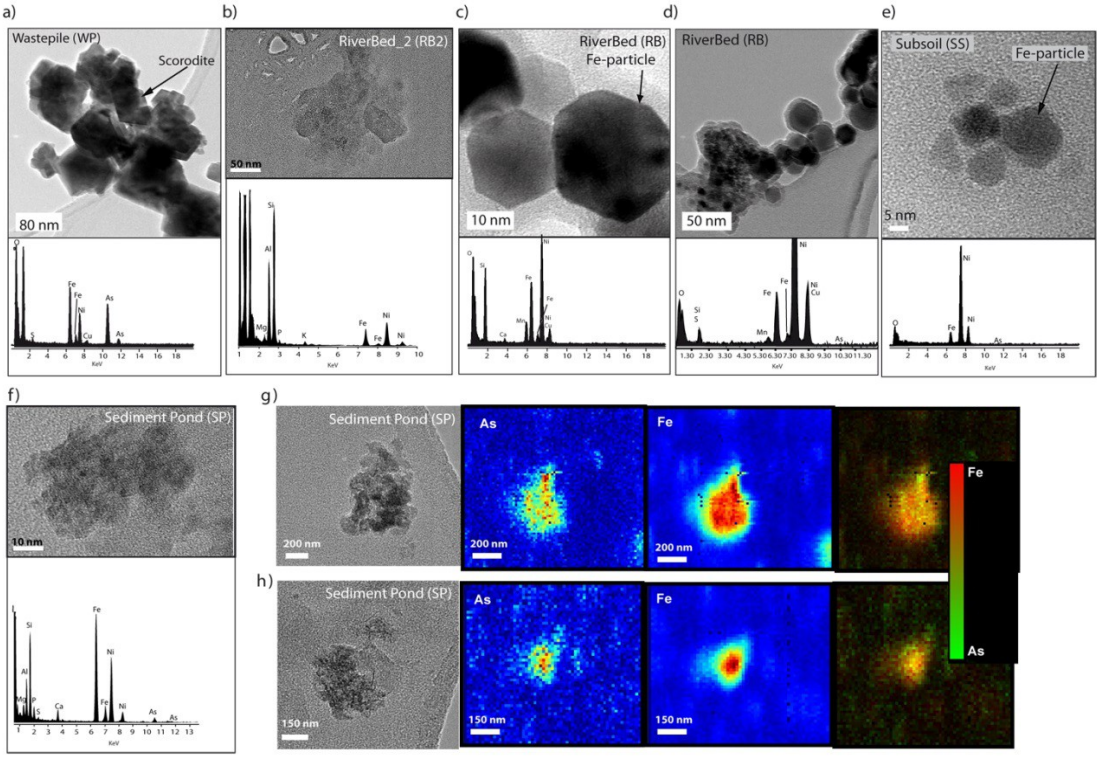

Figure 6: TEM-EDX of colloid fractions. a) scorodite nanoparticle in waste pile, b) aggregates (clay minerals and Fe particles) in riverbed, c) and d) Fe nanoparticles and aggregates in riverbed, e) aggregates of Fe nanoparticles in subsoil, and f) As identified in aggregated of Fe nanoparticles and clay minerals in sediment pond, g) and h) synchrotron µ-XRF element maps of colloid particles in sediment pond downstream.

Conclusions

Contrary to laboratory-based fabrication in other fields, earth sciences samples come from natural, thus uncontrolled sources, which make them highly heterogeneous in most cases. A sub-microfocus beamline gives the opportunity to spatially discriminate the different components giving a more complete picture of the problem to be studied. Of prominent use is the μ-XRF technique to produce chemical maps with a high spatial resolution, but XRD and XAS are also widely used to determine the structure on crystalline or amorphous materials in small scales and concentrations. It is interesting to note that this field can have a strong public impact, as it encompasses the study of toxic elements in contaminated soils, which is a source of major concern.

References

Benzerara, K. Morin, G. Yoon, T.H. Miot, J. Tyliszczak, T. Casiot, C. Bruneel, O. Farges, F. Brown Jr G.E.. *Speciation and solubility of heavy metals in contaminated soil using X-ray microfluorescence, EXAFS spectroscopy, chemical extraction, and thermodynamic modelling* Geochimica et Cosmochimica Acta, 70, 9, 2006, 2163-2190.

Blundy J. and Wood B. *Partitioning of trace elements between crystals and melts*. Earth and Planetary Science Letters 2003, 210: 383-397.

Brown, G. E., Jr., Henricch, V. E., Casey, W. H., Clark, D. L., Eggleston, C., Felmy, A., Goodman, D.W., Grätzel, M., Maciel, G., McCarthy, M.I., Nealson, K., Sverjensky, D. A., Toney, M. F., Zachara, J. M. *Metal oxide surface and their interactions with aqueous solutions and microbial organisms*. Rev. Mineral. Geochem. 2002, 49,1-115.

Brown, G.E. Jr, Struchio N.C. *An overview of synchrotron radiation application to low temperature geochemistry and environmental science*. In: Fenter P.A:, Rivers M. L., Sturchio, N. L. and Sutton S. R (eds.) Applications of Synchrotron Radiation in Low- Temperature Geochemistry and Environmental Science. Review in Mineralogy and Geochemistry 49: 1-115.

Elzinga, E.J., Reeder, R. J. *EXAFS study of Cu^{2+} and Zn^{2+} adsorption complexes at the calcite surface-Implications for site-specific metal incorporation preferences during calcite crystal growth.* Geochimica et Cosmochimica Acta 2002 66, 3943-3954.

Galoisy L., Calas G., Arrio, M. A. *High-resolution XANES spectra of iron in minerals and glasses: structural information from the pre-edge region*. Chemical Geology, 174, (1-3) 2001, 307-319.

Helmhart M., Serrano S., Garrido F., O'Day, P.A. *Impact of preferential flow on arsenic distribution and speciation in an alluvial sediment from São Domingos mine (Portugal)* Unpublished (2014)

Isaure M P, Fayard B, Sarret G, Pairis S, Bourguignon J.. *Localization and chemical forms of cadmium in plant samples by combining analytical electron microscopy and X-ray spectromicroscopy*. Spectrochimica Acta-Part B Atomic Spectroscopy, 2006 61, 1242-1252**.**

Kamenos N.A., Cusack M., Huthwelker T., Lagarde P., Scheibling R.E. *Mg-lattice associations in red coralline algae*. Geochimica et Cosmochimica Acta 2009, 73,1901–1907.

Kirpichtchikova, T. A. Manceau, A. Spadini, L , Panfili, L., Marcus, M. A., Jacquet. T. *Nanoscale study of As biomineralization in an acid mine drainage system.* Geochimica et Cosmochimica Acta, 72, (16), 2008, 3949-3963.

Luster J., Göttlein A., Nowack B., Sarret G., 2008, *Sampling, defining, characterising and modelling the rhizosphere - The soils science toolbox*, Plant and Soil, 321 (2009) 457-482

Manceau A., Nagy K.L., Marcus M.A., Lanson M., Geoffroy N., Jacquet T., Kirpichtchikova T.: *Formation of metallic copper nanoparticles at the soil-root interface.* Environmental Science and Technology, 42, 1766-1772.

Maurice P. A., Hochella, M. F. *Nanoscale Particles and Processes: A New Dimension in Soil Science*. In: Advances in Agronomy, Chapter 5, 100, 2008, 123-153.

Metrich N., Bonin-Mosbah M., Menez B., Galoisy L. *Presence of (S4+) in arc magmas: Implications for volcanic sulfur emissions*. Geophysical Research Letters 29: 014607.

Ona-Nguema, G., Morin, G.,Wang, Y., Menguy, N., Juillot, F., Olivi L., Aquilanti G., Abdelmoula M. , Ruby, C., Bargar, J. B., Guyot, F., Calas, G., Brown, G. E. Jr. *Arsenite sequestration at the surface of nano-Fe(OH)$_2$, ferrous-carbonate hydroxide, and green-rust after bioreduction of arsenic-sorbed lepidocrocite by Shewanella putrefaciens*. Geochimica et Cosmochimica Acta, 73, (5), 2009, 1359-1381

Parise, J. B. and Brown, G. E. Jr. *New opportunities at Emerging Facilities*. Elements, 2, 2006, 37-42.

Reeder, R. J., Nugent, M., Tait, C. D: Morris, D. E., Heald, S.M., Beck, K. M., Hess, W.P. and Lanzirotti, A. *Coprecipitation of uranium (VI) with calcite: XAFS, micro-XAS, and luminescence characterization*. Geochimica et Cosmochimica Acta 2001 65, 3491-3503.

Sarret G., Balesdent J., Bouziri L., Garnier J. M., Marcus M. A., Geoffroy N., Panfili F., and Manceau A. (2004) *Zn speciation in the organic horizon of a contaminated soil by micro X-ray fluorescence, micro and powder EXAFS spectroscopy and isotopic dilution.* Environ. Sci. Technol. 38, 2792-2801

Schlegel M. L., Manceau, A. *Evidence for the nucleation and epitaxial growth of Zn phyllosilicate on montmorillonite*. Geochimica et Cosmochimica Acta, 70, (4), 2006, 901-917.

Serrano S., Gómez-González, M.A., O'Day, P.A., Laborda F., Bolea, E., and Garrido, F. *Arsenic speciation in the dispersable colloidal fraction of soils from a mine-impacted creek*. Unpublished (2014)

Tang Y., Chappel H. F., Dove M. T., Reeder R. J., Lee Y. J. *Zinc incorporation into hydroxylapatite.* Biomaterials, 30, (15), 2009,2864-2872.

Cultural heritage

Spain has got a considerable amount of relevant cultural heritage objects belonging to different key periods of human history in numerous top world ranked museums and sites. Their study involves a wide range of non destructive and non invasive techniques, sometimes applied on unique masterpieces, to improve the understanding of their manufacture, their evolution and/or degradation during time. This understanding is necessary to give a basis either for the reconstruction of the past or for the restoration and conservation of objects to safeguard our common history for future generations.

Third generation synchrotrons sources played a central role in developing cultural heritage science thanks to beamlines with microfocussing capabilities that provide a high spatial resolution down to 1 μm coupled with a high photon flux allowing to achieve low detection limits down to ppb. These specifications fulfil most of the experimental needs on cultural heritage where samples are heterogeneous and limited i.e. standard painting cross sections with layers about 50-500 μm thick each containing pigments about 1-10 μm in diameter.

The samples can be crystalline, amorphous and/or diluted in nature; they are diverse as diverse are the materials constituting our cultural heritage. Some sample examples include pigments, bones, ceramics, metals, plasters and mortars, glasses, wood, faded inks and layers on parchments and canvas. Chemical and structural information on these materials are required by the researchers and can be provided by means of μ-XRF, μ-XRD and μ-XANES/EXAFS. Since these materials appear routinely mixed in the same sample these techniques are used mostly in a combined fashion rather than separately.

The understanding of cultural heritage objects involves an interdisciplinary collaboration between archaeology, art history and preservation of the cultural heritage, ethnography and material science. Routinely any research starts with the characterization of the component materials and then some information can be extrapolated regarding the identification of its creative process, the evaluation of the alteration processes, the diagnosis of previous modifications and dating. This information is extremely valuable to the conservator and restorers for preventive conservation on one hand, and to the archaeologists to identify the provenance, manufacture and function of a wide range of objects on the other.

The use of synchrotron techniques on a wide range of cultural heritage related problems has experienced an exponential growth in terms of the amount of scientific papers published since early 90's until the end of 2008, as shown on Pantos (2008). In parallel, the use of synchrotron radiation by different Spanish researchers on ancient objects attracted the attention of the media and have had and extended press coverage as seen on M. Vendrell-Saz (2006). Nowadays there are several Spanish groups involved in research projects using synchrotron radiation on cultural heritage.

This well established community of users has become pioneer in applying synchrotron microfocussing techniques on ceramics and paintings as a new way to characterize uniequivoquely component materials on altarpieces, to unveil the creative process of medieval lustre ceramics and understand the decay processes involved in mural paintings. These scientific cases provide good examples about all the potential that a microfocus beamline can provide when applied on art and archaeological objects.

Characterization of component materials

Identifying the components constituting an art object is one of the major challenges faced in

cultural heritage and can provide important hints about its preventive conservation, dating and provenance. Paintings are one of the most important art objects since they are directly linked to the self representation of societies from across all the epoques and have been object of a great number of such studies. Microfocus techniques applied on Spanish paintings have revealed to have a huge potential in elucidating the nature and distributions of pigments within the chromatic layers, and have been used to reveal the phases and composition of green copper pigments on Catalan Gothic altarpieces. Moreover they have been used to identify the pigments present in mural paintings from San Austin's Church in Cordoba and to identify the pigments used by the artist Pedro Anastasio Bocanegra on a series of canvas depicting the life of San Ignacio.

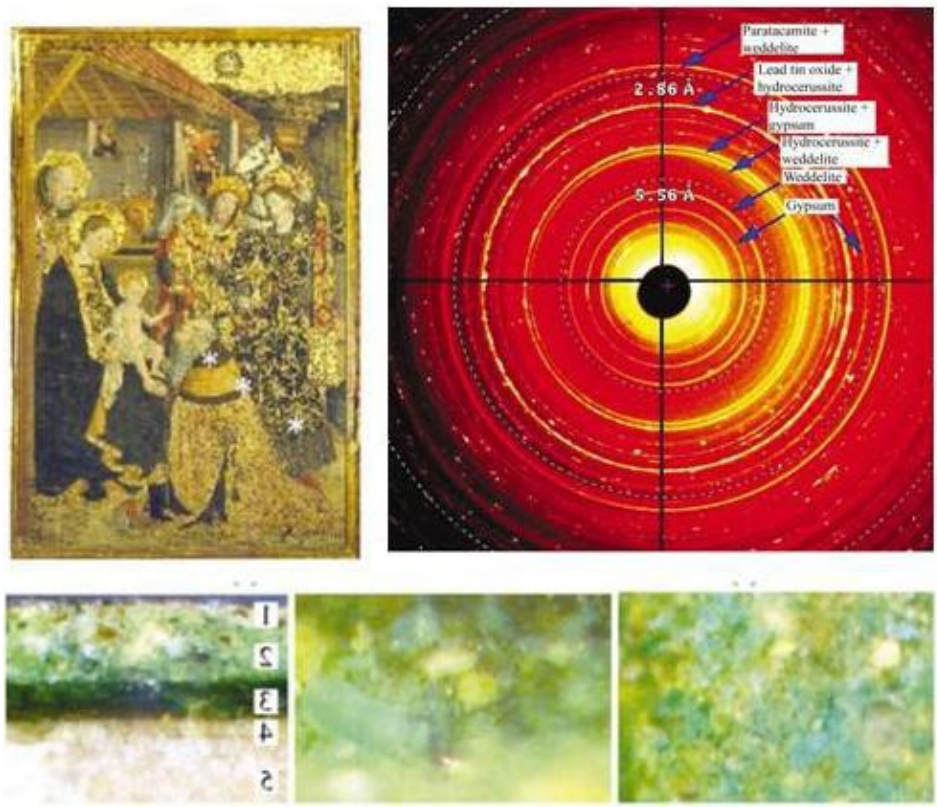

Figure 7: Jaume Huguet gothic paintings and the corresponding chromatic layers containing green copper based pigments and the associated powder diffraction rings obtained on one of the layers.

Synchrotron radiation was used by N. Salvado et al. (2002) to identify the copper green pigments used by one of the most important Catalan masters in Gothic paintings from the 15th century, Jaume Huguet. Synchrotron radiation μ-XRD combined with other spectroscopic techniques was used to produce maps of phases at a spatial resolution of 100 μm across chromatic layers. Ancient synthetic copper-based green pigments were compounds obtained by the corrosion of copper or copper alloys exposed to vinegar. The process used in antiquity is described by ancient authors, although there was not much conclusive evidence of their application on paintings and no detailed study had been undertaken on the copper compounds used and the connection with different manufacturing techniques. Some of the most important altarpieces of Jaume Huguet were sampled as seen in Figure 7. The green pigment turned to be heterogeneous in size with diameters ranging from 1 to 10 μm, with different morphologies

and colours (dark green, light green, blue) and the results obtained on real samples were compared to green copper pigments synthesized in the laboratory under controlled conditions. In this work it was demonstrated that a mixture of different copper based compounds, such as acetates $Cu(CH_3COO)_2 \cdot H_2O$, basic chlorides $Cu_2(OH)Cl_3$, $Cu(OH,Cl)_2 \cdot 2H_2O$ and carbonates $Cu_2CO_3(OH)_2$, $Cu_2CO_3(OH)_2$ constituted the copper green colours in the altarpieces and stated that Jaume Huguet used a green pigment which was synthesized following a procedure that consisted of coating copper plates with honey and salt and exposing them to vinegar vapours in a sealed receptacle.

X-ray microdifraction carried out at MSPD beamline at ALBA, has provided novel information concerning the composition and crystalline phases present in a selection of grisailles from several cathedrals in Spain (Avila, Burgos, Alcalá de Henares and Segovia) dating from the 15th to the 19th century made by several master glaziers were studied (Figure 8). A grisaille is a brown-blackish paint applied onto the inner surface of stain glass to draw the contours of the figures. They were traditionally made of finely ground oxides of iron but also of copper, zinc, lead or manganese mixed with lead ground glass. The micrometer layer structure of the grisailles, (typical layer thicknesses vary fromo 10 to 100 micrometer) together with the low amount and diverse nature of the compounds(pigment particles, crystalline and amorphous compounds, aging and weathering compounds) have limited their indentification up to now. Changes from the methods of production and materials in the different historical periods are obtained and also related to the conservation state of late materials.

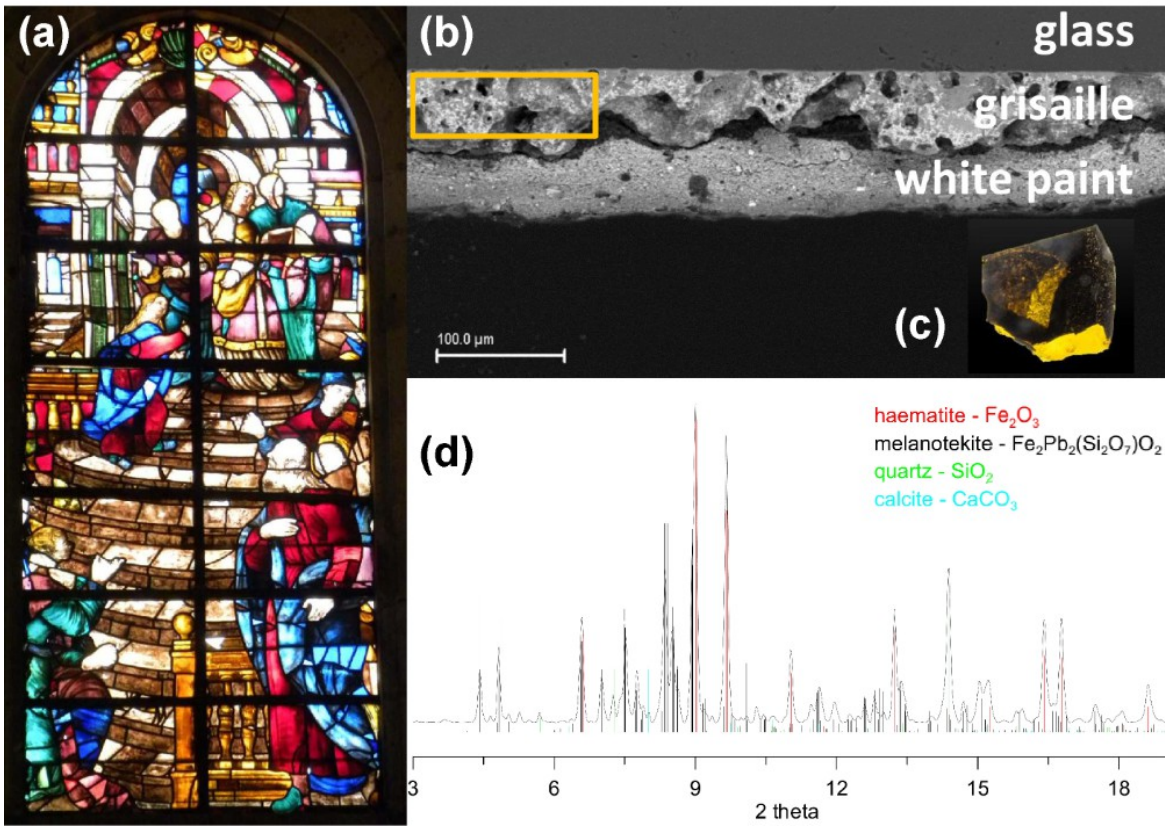

Figure 8: (a) Studied stain glass window. (b) SEM micrograph of a fragment of a yellow piece (c), showing the grisaille. (d) XRD diagram showing the different components

Micro X-ray diffraction (μ-XRD) has been used by L.K. Herrera et al. (2008) as well to identify pigments from the chromatic layers of two samples taken from wall paintings at San Agustin's Church in Cordoba. Crystalline iron oxide phases such as goethite, lepidocrocite and hematite in the cross-section of the painting thin layers were identified, with a good spatial resolution, while laboratory XRD only detected hydrocerussite and cerussite rather than the full range of iron phases found in the μ-XRD experiments. Furthermore, combining μ-XRD and μ-XRF has been proved a powerful methodology to identify pigments [L.K. Herrera et al., 2009] from six famous canvases painted by Pedro Atanasio Bocanegra, who created a very special collection depicting the life of San Ignacio, which are located in the church of San Justo y Pastor of Granada in Spain. In this work characterization of the inorganic and organic compounds of the textiles, preparation layers, and pictorial layers have been carried out using μ-XRD and μ-XRF so a new pigment (monazite, $CeLaPO_4$) has been identified. [Pradell et al, 2014]

Identification of the creative process

The understanding of how ancient objects were produced gives us the chance to infer how the past societies used and shared technologies giving us hints of their interaction and development. Ceramic pots and plates are one of the most significant physical remains since early stages of human civilizations and their study gives us the opportunity to elucidate the distribution, technological development and connections amongst ancient societies. The ceramic production reached its maximum point of complexity and sophistication with lustre decorated ceramics, a ceramic decoration constituted by copper and silver nanocrstyals embedded inside a glassy matrix that probably was developed in Irak during the 9th century and spread all across the western Mediterranean with the expansion of the Islamic culture. Spain had some of the most significant Islamic lustre ceramic production centers such as the archaeological sites from Paterna in the SE of Spain with important ceramic remains that have been extensively studied using synchrotron radiation techniques.

The study of lustre production from the Olleries Xiques archaeological site in the city of Paterna has been performed by using μ-XRF, μ-XRD and μ-XANES/EXAFS. This site dates back from the 12th century and was an important district in Paterna densely populated of ceramic kilns exclusively dedicated to glazed ceramic production. During the 13th century the city was conquered by the Aragon Crown and occupied by the Christians, however the ceramic production did not stop and produced huge amounts of lead glazed ceramics decorated with lustre and was exported all across the Mediterranean. For their study and comparison ancient ceramic fragments on site were provided by the local archaeologists and modern lustre reproductions produced in the same way as their ancient ceramists counterparts had been obtained from a local workshop. These studies stated that copper and probably silver were introduced inside the glassy matrix by means of an ionic exchange between a raw paint and the alkalis from the glass during annealing in a reducing atmosphere [T. Pradell et al., 2006, and J. Roque et al., 2007].

The μ-XRF and μ-XANES/EXAFS in Figure Error: Reference source not found showed that aesthetic heterogeneities on the decorations correspond to silver and copper variations being copper and silver anticorrelated inside the glassy matrix in terms of chemical composition and oxidation state A.D. Smith et al 2006. Lustre final optical properties had been partly revealed as well by means of μ-XRD and TEM linking the accumulation and development of metallic nanoparticles inside the glass matrix to its characteristic shine and colour [J. Roqué et al. 2006]. By combining the microfocusing synchrotron radiation

techniques with TEM microscopy and comparing the modern lustre productions with the archaeological ones it was found that the huge accumulation of ceramic left over the Olleries Xiques site corresponded to defective productions with remarkable amounts of oxidized nanoparticles as they probably did not fulfil the required aesthetic standards.

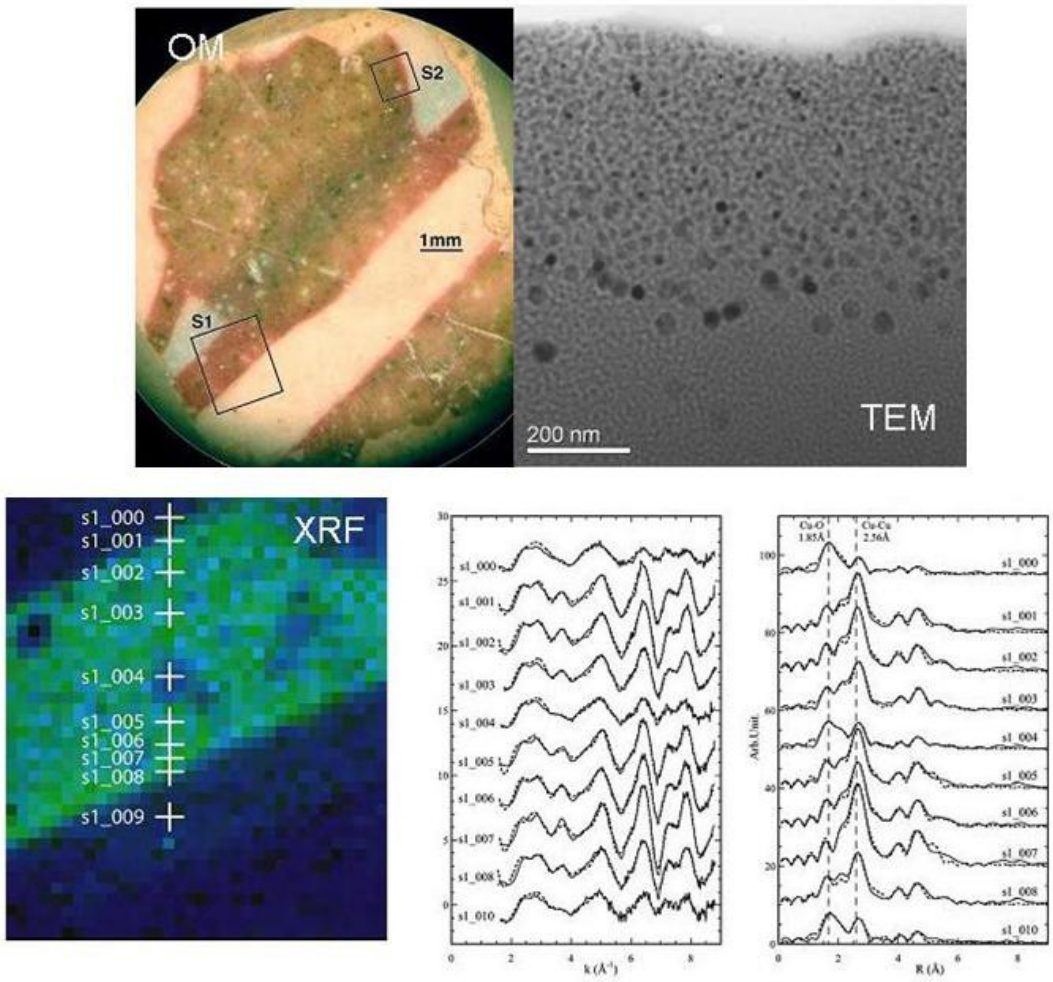

Figure 9: (top) Ceramic lustre from Paterna (Spain). Sampled region and TEM pictures showing copper nanoparticles. (bottom left) XRF mapping for Cu-Kα. (bottom right) Cu-K edge EXAFS spectra obtained across the lustre decoration and magnitude of the Fourier Transform of the EXAFS spectra.

Evaluation of the alteration processes

Environmental conditions have a significant effect on the appearance and properties of the objects constituting our cultural heritage. Exposure to weather and atmospheric pollutants affect stained glasses, burial affects the structure of glasses, bones, ivory and wood, photo-oxidation and photo-degradation occurs on varnishes, dyes, pigments, organic media, glues, paper and textile components and climate conditions can degrade stones through the actions of freezing, lixiviation, pollution and corrosive gases. There are several examples in the literature about applying microfocus synchrotron techniques to understand the weathering

process occurring on art objects specially dealing with the darkening and fading of colours, these studies are generally focussed on either the changes affecting the binding media or the pigments within the chromatic layers. Other works are more orientated to the preservation of the structure of the objects themselves, this include examples regarding the study of corrosion processes occurring on metal pipes from Spanish baroque organs and the study of the acidification processes that take place in archaeological wood from sunk vessels.

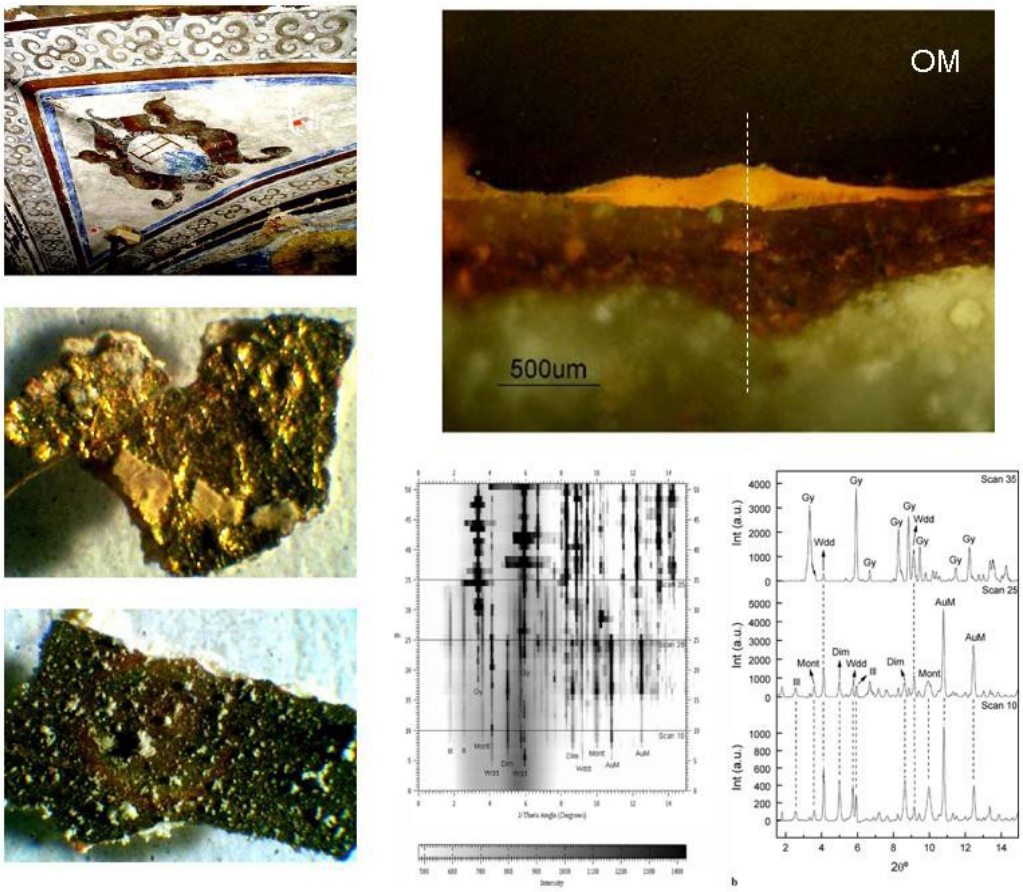

Figure 10: 17th century gilded paintings from the crypt of Sant Benet de Bages. (Top left) Unaltered and weathered sample. (Top right) cross section from the weathered sample and (bottom right) the associated μ-XRD line scan through all the chromatic layers showing the distribution of pigments. (Middle left) gold leaf and (bottom left) the oxalate weddellite.

A. Lluveras et al. (2007) applied synchrotron microfocus techniques to identify weathering by-products from a medieval monastery near Barcelona. This research dealt with the causes leading to the darkening of the gilding sample and its decay processes compared with other gilding samples which remained unaltered. Samples of both types of gilding were collected and analysed by a combined use of conventional techniques as seen on the Figure 10. Since traditional techniques did not fully solve the problem in relation with the differential ageing of the gilding samples, synchrotron techniques were deployed in order to obtain information on the weathering process. Synchrotron radiation X-ray diffraction was used to produce line scans of phases across chromatic layers. The μ-XRD profiles allowed obtaining information on the distribution of compounds and added information to the standard laboratory based characterisation results. The calcium oxalate weddellite (wdd in Figure 10) distribution

demonstrates the relationship between the presence of binding medium and its development, and from these preliminary results it appears that the hypothesis considering calcium oxalates as a deposition of materials from a biomineralisation process or from pollution could be discarded and instead should be related to the presence of the organic binding material itself. However it seems that the presence of the gold leaf prevented the normal exposition to light and oxygen of the mordant and thus the development of calcium oxalates whilst in the water gilding decoration made on a bol lost its golden aspect due to the decay of the organic material linked to a huge development of calcium oxalates.

However not only μ-XRD has been revealed as a powerful tool to identify pigments and the associated decay products within the chromatic layers, there are other studies that use instead μ-XANES spectral signature to identify this type of compounds. This is the case of M. Cotte et al. (2006) that used the S K edge μ-XANES in parallel with μ-XRF to characterise weathered red pigments from Pompeii. The samples were studied in a fluorescence set up and the spectral signature of S K edge μ-XANES obtained on the paintings is compared to those obtained on a selected range of standards of mercury sulphide compounds and natural minerals. Afterwards the information obtained was crossed with the chemical distribution of Cl and S to identify the nature of the decay products. This work identified vermillion as the main pigment used and its darkening effect seemed to be affected by the interaction of the chromatic layer with some exogenous Chlorine.

The corrosion process and distributions of major elements, lead and tin, as well as the identification and distribution of trace elements present in the tin and lead phases of metal pipes of a Spanish baroque organ were studied with the aid of microfluorescence [L. K. Herrera et al., 2009]. It was found that the major elements were totally segregated and that the trace elements, Fe, Ni, Cu and Hg, were located within the lead phase. Moreover the presence of a new phase, laurionite, including chlorine, was identified in the surface region. This degradation product of lead was probably formed during the cleaning processes using bleach.

Other studies are focussed on the conservation of wood like in the Mary Rose, a sunken warship from the 16th century affected by an acidification process that has been studied in K.M. Wetherall et al. (2008) by means of sulphur and iron K-edge μ-XANES. Results from sulphur K-edge μ-XANES reveal that the concentration of highly oxidized sulphur decreases with depth into the timber. Iron K-edge μ-XANES reveals little variation with depth in which Fe^{3+} ions are dominant. This gives some light on the sulphur oxidation path suggesting that Fe^{3+} ions are produced by the oxidation mechanisms that are currently underway.

Conclusions

A microfocus absorption spectroscopy beamline from low to middle energies, with micro diffraction capabilities, would provide a full range of new experimental possibilities allowing achieving an ultimate understanding of the chemical and structural properties from the art objects and has a huge potential in helping to elucidate a wide range of problems related to their history and conservation. A microfocussing beamline proved to be highly versatile and especially suitable for the sampling methodologies needed on a wide range of art objects from paintings to ancient ceramics and archaeological wood. Since Spain has been a junction of cultures, societies and religions for centuries, it has a rich historical record with important sites and art examples, a synchrotron microfocus beamline combined with this diversity and cultural richness would help to consolidate the Spanish scientific community at the top of the world research ranking in Cultural Heritage and related disciplines.

References

A.D. Smith, T. Pradell, J. Roqué, J. Molera, M. Vendrell-Saz, A.J. Dent and E. Pantos *Color variations in 13th century hispanic lustre – An EXAFS study* Journal of Non-Crystalline Solids 2006 352 5353-5361

A. Lluveras, S. Boularand, J. Roqué, *Weathering of gilding decorations investigated by SR: development and distribution of calcium oxalates in the case of Sant Benet de Bages (Barcelona, Spain)* Applied Physics A 2007 90(1) 23-33

L.K. Herrera, M. Cotte, M.C. Jimenez de Haro, A. Duran, A. Justo, J.L. Perez Rodriguez, *Characterisation of iron oxide-based pigments by synchrotron-based micro X-ray diffraction.* Applied Clay Science **42** (2008) 57-62.

L.K. Herrera, S. Montalbani, G. Chiavari, M. Cotte, A.V Solé, A. Duran, A. Justo, J.L. Perez-Rodriguez *Identification of pictorial materials from Bocanegra paintings*. Talanta **80** (2009) 71-83..

L.K Herrera**,** A. Justo, J. A. Sans, G. Martínez-Criado, A. Muñoz-Paez *Chemical composition of the metal pipe of a Spanish baroque organ as determined by μXRF.* Analytical and Bioanalytical Chem. 395 (2009) 1969-1975.

J. Roqué, J. Molera, P. Sciau, E. Pantos and M. Vendrell-Saz. *Copper and silver nanocrystals in lustre lead glazes: Development and optical properties* Journal of the European Ceramic Society 2006 26(16) 3813-3824.

J. Roque, J. Molera, J Perez-Arantegui, C. Calabuig, J Portillo, M Vendrell-Saz, *Lustre colour and shine from the olleries xiques workshop in paterna (Spain), 13th century Ad : Nanostructure, chemical composition and annealing conditions* 2007 Archaeometry **49** 511-52.

K.M. Wetherall, R.M. Moss, A.M. Jones, A.D. Smith, T. Skinner, D.M. Pickup, S.W. Goatham, A.V. Chadwick and R.J. Newport *Sulfur and iron speciation in recently recovered timbers of the Mary Rose revealed via X-ray absorption spectroscopy* Journal of Archaeological Sciences 2008 35(5) 1317-1328

M. Cotte, J. Susini, N. Metrich, A. Moscato, C. Gratziu, A. Bertagnini and M. Pagano *Blackening of Pompeian Cinnabar Paintings: X-ray Microspectroscopy Analysis* Analytical Chemistry 2006 78 7484-7492.

N. Salvadó, T. Pradell, E. Pantos, M. Z. Papiz, J. Molera, M. Seco and M. Vendrell-Saz *Identification of copper-based green pigments in Jaume Huguet's Gothic altarpieces by Fourier transform infrared microspectroscopy and synchrotron radiation X-ray diffraction* Journal of Synchrotron Radiation 2002 9 215-222

Patrimoni-UB Recull de Premsa. *La luz Sincrotron Ilumina obras de arte* [on line]. Barcelona, Spain: M. Vendrell-Saz, 29 May 2006 [Read: 18 March 2009]. Available: <http://161.116.85.21/patrimoniUB/>.

SRS Daresbury. *STFC Heritage Science* [on line]. Daresbury, UK: E. Pantos, 4 September 2008 [Read: 18 March 2009]. Available: <http://srs.dl.ac.uk/arch/publications.html>.

T. Pradell, J. Molera, J. Roque, M. Vendrell-Saz, A. D. Smith, E. Pantos and D. Crespo *Ion-exchange mechanisms in the formation of medieval luster decorations* 2006 Journal of the American Ceramic Society **88**, 1281-1289.

T. Pradell, G. Molina, S. Murcia, J. Molera, in Synchrotron Radiation and neutrons in art and archeology Conference, Louvre, Paris (September 2014)

Materials science

The last years have seen a significant growth in the application of X-ray microscopy in different areas of materials science. Regardless the analytical probes, the major goal is to achieve a deep understanding of the relationship between structure, processing and underpinning properties of materials. For both research and industrial evaluations, the microscopic studies are intended to reveal the degradation mechanisms, elemental traces, short/long range structural order formation and driving forces of failure processes as well as doping-induced defects in synthesized components. Their role in the emerging technology and the resulting device performance is crucial to overcome current engineering problems.

Today, modern electron-optical instruments are able to a spatial resolution better than 0.5nm. However, it is necessary to complement the morphological information with chemical, structural and optical analysis of certain sample regions in order to determine the relationship between crystallographic changes and compositional variations of the different components on the very same micrometer scale. Synchrotron-based microscopy fulfils these needs by providing an in-situ means of identifying elements within micro-volumes of samples with a very high degree of sensitivity and site selectivity. Its high-demand stems from its capability of obtaining elemental images with simultaneous chemical and structural analysis for a very wide range of materials by a non-destructive way. This requires a combination of a high brilliance X-ray source with long working distance achromatic optics incorporated without compromising the sample examination in the X-ray fluorescence and diffraction detection modes. Thus, the X-ray microprobe has become an indispensable tool for spatial resolved characterization of materials with micrometer resolution (e.g. precipitates, clusters, segregation effects).

The broad range of materials types and applications ussually leads to subdivide this field into “hard” and “soft” materials, with their own characteristics. The scientific cases included below illustrate the capabilities of the microfocus techniques on both subfields.

Materials science: hard condensed matter

Hard condensed matter generally deals with materials with structural rigidity, such as crystalline solids, glasses, metals, insulators, and semiconductors, generally inorganic. The term hard matter is commonly used to refer to matter governed by atomic/molecular forces and quantum mechanics. This is probably the most traditional field on materials science, and its range of applications is large and varied. It follows a few examples already published from Spanish research groups on the use of synchrotron microprobes on these kind of materials.

Impurity clustering and local structural order in semiconductors

Deep-ultraviolet-transparent conducting oxides (DUV-TCO) are becoming a subject of increasing technological interest in several fields. In particular, as the emission of DUV light emitting diodes (LED) shifts to shorter wavelength, DUV-TCO will be needed in vertical-cavity surface-emitting configurations. Efficient DUV-TCOs will be also required in DUV photo detectors and imaging-arrays, in antistatic electric layers in DUV photolithography or in "lab-on-a-chip" devices for DNA and protein analysis. The most commonly used TCOs, like Ga- or Al-doped ZnO and ITO have an optical gap of around 4 eV and absorb DUV radiation. It has been shown that Ga doped rock-salt ZnO behaves as a DUV-TCO, with a band gap of 5 eV and resistivitity below 10^{-3} Ωcm, indicating that Ga atoms behave as donor in rock-salt ZnO and proposed Ga-doped rock-salt $Zn_{1-x}Mg_xO$ ($x>0.4$) as a good candidate for DUV-TCO.

But, it has also been displayed that heavily Ga-doped wurtzite ZnO, with an optical bandgap of 4 eV and resistivities as low as 10^{-4} Ωcm, contains a large amount of electrically inactive Ga atoms. Where are these atoms? By means of micro-X-ray absorption spectroscopy, a study of the site configuration of Ga atoms in Ga-doped ZnO thin films [Sans et al., 2007a] shows that Ga-related donors remain electrically active after vacuum annealing at 800 °C. On the opposite, annealing the films in air (400 °C) leads to a dramatic decrease of the conductivity by four orders of magnitude and disappearance of the Burstein-Moss shift. μ-XAS spectra indicate that air annealing induces partial segregation of Ga atoms to nanocrystallites of the spinel $ZnGa_2O_4$ or other intermediate phases. The short Ga–O bond length measured can be at the origin of the reported instability.

Magnetic semiconductors for spintronics

There have been an extensive experimental searches for spintronic materials among dilute magnetic semiconductors in particular GaN and ZnO doped with transition metals. The magnetic properties have shown completely different results. The variety of experimental factors affecting the magnetic properties include the apparition of multiple phases (zincblende, wurtzite, spinel), transition metal clustering or nanophase formation, substitutional versus interstitial doping, mixed valences, strains induced by the substrate or the presence of inhomogeneities. Micro XAS has been used in Mn doped GaN to assess these problems [Martínez Criado et al. 2004, 2005; Sancho-Juan et al. 2006, 2009, 2011]. It has been shown that GaN:Mn grown by molecular beam epitaxy on SiC substrates presents homogenous Mn distribution. Mn is substitutional in the wurtzite structure, acquiring tetrahedral coordination and an ionization state very close to +2. In the same line there have been studies carried out in Co (Figure 11), [Martínez-Criado et al., 2004] and Mn doped thin films [Pellicer-Porres et al., 2006; Sans et al., 2007b, Sans et al., 2010; Gilliland et al., 2010] and nanowires [Segura-Ruiz et al., 2011]. In Mn doped ZnO thin films the local structure around Mn has been studied both in the wurtzite phase and in the high pressure rocksalt polymorph. It has been shown that Mn substitutes Zn in both phases (Figure 12).

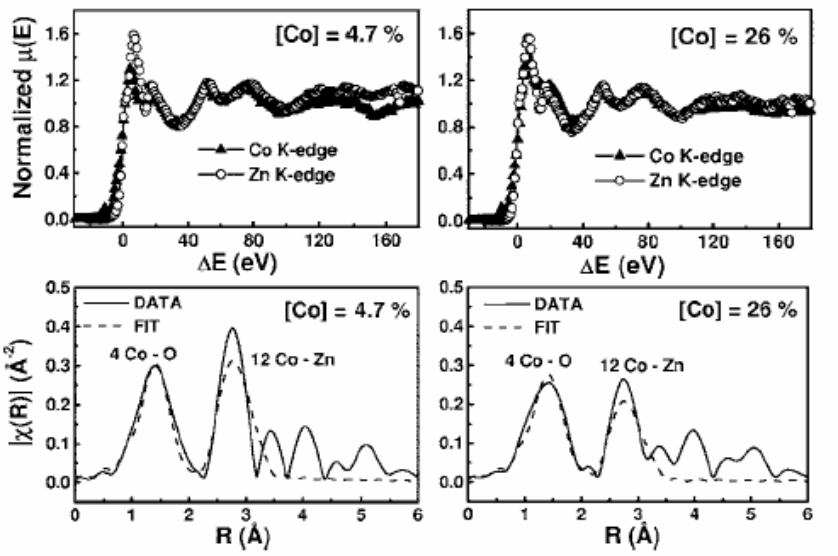

Figure 11: Upper part: Comparison of the Co and Zn K-edge XANES spectra for Zn1−xCoxO with two different Co contents: 4.7% and 26%. Lower part: Comparison of the Fourier transforms of the Co K-edge EXAFS functions for two different Co contents: 4.7% and 26%.

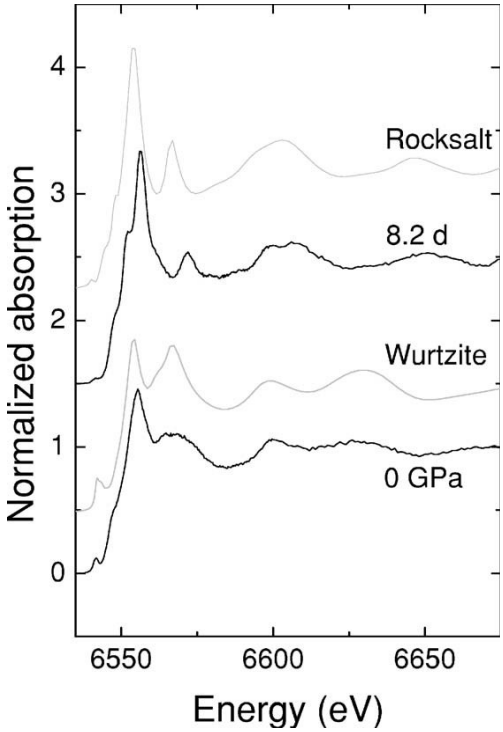

Figure 12: Comparison between experimental ZnO:Mn spectra and multiple scattering XANES simulations based on a structural model where Mn would occupy the Zn site. The simulations are performed both in the low pressure wurtzite phase and in the high pressure rocksalt phase.

Nanotechnology: location of dopants in nanowires

The work on nanowires gives an idea of the broad range of possibilities offered by a μ-XAS beamline. First of all the material under study has micrometric dimensions. The composition homogeneity of such small objects has to be checked.

In Figure 13, a $Zn_{1-x}Co_xO$ nanowire is studied by μ-XRF mapping to evaluate the homogeneity of the Co doping [Segura-Ruiz et al., 2011]. Furthermore, it is possible to take profit of the anisotropy of the sample and the polarization of synchrotron radiation to analyze the XANES fingerprints indicating the Co substitutional character. The work is done at the Zn and Co K-edges even if the Co concentration is as low as 0.3 atom %.

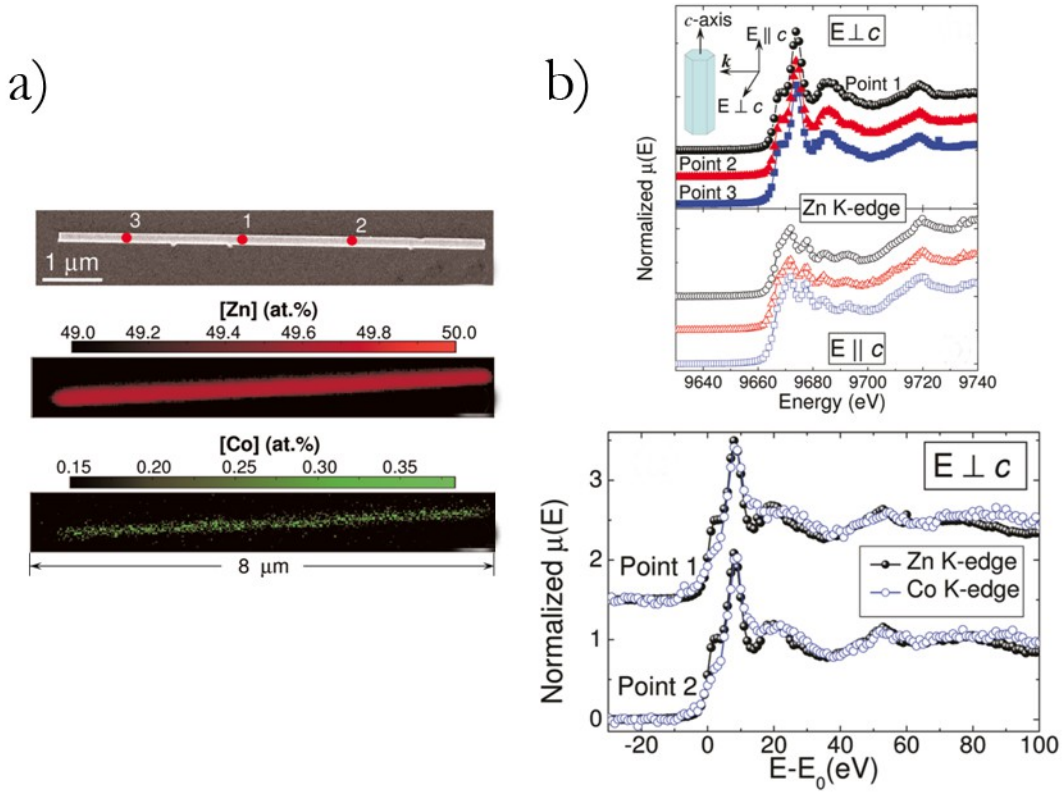

Figure 13: µ-XAS characterization of Co doped nanowires. a) Fluorescence study showing the chemical homogeneity of the nanowires. b) The Co substitutional character is demonstrated by polarized XANES spectra at the Zn and Co K-edges

A second example on semiconductor nanowires are Mn_x- and In_x- $Ga_{1-x}N$ samples. Several samples of GaN with different Mn content were studied by µ-XRF and µ-XAS to extract information about the elemental distribution at the nanowire and the valence of Mn, respectively. In Figure 14 (left) the XRF spectra can be seen, taken at an excitation energy of 12 keV and at an incident angle of 45 degrees, of the different samples with a Mn nominal content of 3.85, 6.57, 6.92 and 8.76 %. The K-peaks of Mn and Ga are clearly shown, allowing a quantification of the Mn and Ga content in the samples.

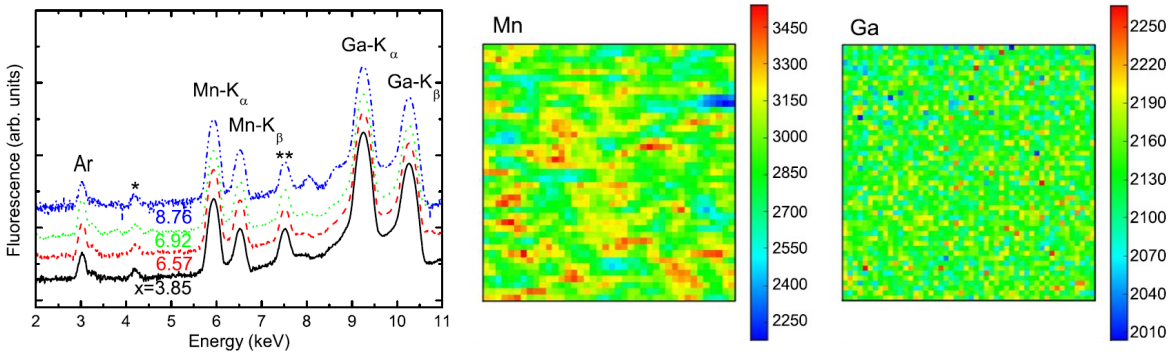

Figure 14: (left) XRF spectra for the different Mn concentrations on the $Mn_xGa_{1-x}N$ nanowire. (right) µ-XRF mapping of the inside of a nanowire, in a 50 x50 μm^2 area.

Furthermore, XRF of the different samples was measured in a small area, around 50×50 μm^2. (Figure 14 (right)) The beam resolution was around 40-50 nm. In the figure below it is shown the Mn and Ga distribution in the more inhomogeneous sample, with a 8.76% of Mn. The scales are in arbitrary units.

We can see that the distribution of Mn is quite homogeneous, with small areas showing a lower Mn content or very small areas with higher Mn content. It has been also shown [Sancho-Juan et al., 2009] from the EXAFS experiments that the Mn substitutes the Ga and that the valence of Mn is between +2 and +3, closer to +2. The position of the XANES spectrum was analyzed carefully and the peaks were related with band to band transitions by comparison with ab initio calculations.

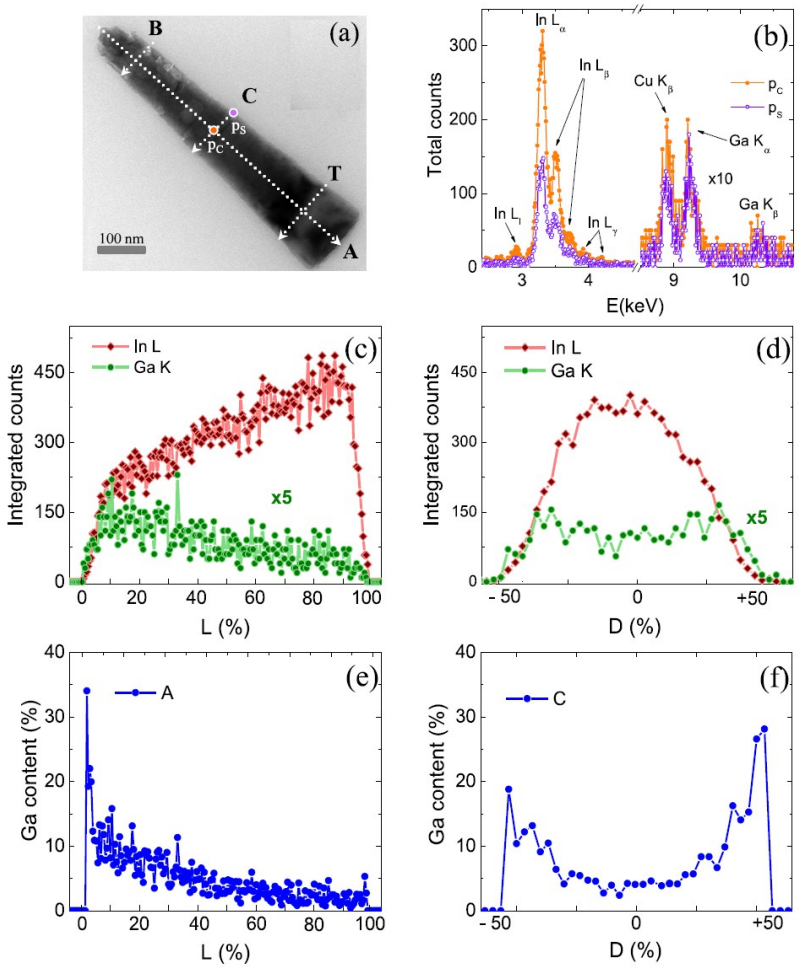

Figure 15: (a) HRTEM image of one of the InGaN nanowires, showing the A, B, C and T directions, where the μ-XRF scans were made, and the P_C (core) and P_S (shell) points where XRF spectra were measured. (b) the fluorescence at P_C and P_S are shown, where the difference in In and Ga content can be seen. (c) and (d) show the integrated fluorescence (K and L lines of Ga or In, respectively) along the nanowire (A direction) and perpendicular to it (C direction). (e) and (f) show the Ga relative content along the A and C axes measured by HRTEM-EDX confirming the XRF measurements

In the study of InGaN nanowires, the In and Ga content was analyzed [M. Gómez-Gómez et al., 2014]. HRTEM-EDX and XRF were combined to extract the amount of Ga and In in

the sample. The first technique has a better spatial resolution while the second has a strong sensitivity due to the luminosity of the synchrotron source.

In figure 15(a) one of the nanowires and the different scans done on it (A, B, C and T directions, and the points PC, indicating the core, and PS, indicating the shell) are shown. In (b), the fluorescence at PC and PS is shown, where we can appreciate the difference in In and Ga content. In (c) and (d) scans, a larger amount of In in the core, as compared to the shell can be observed. This means that there is a spontaneous formation of core-shell nanowires during the fabrication process. Also, the amount of Ga decreases from the bottom to the top of the nanowires. In the last graphs (e and f) it is shown the equivalent to (c) and (d) measured with HRTEM-EDX.

In-situ studies: high pressure

In the high pressure community the words “high pressure” are reserved to pressures above 100 MPa (1 kbar) [Menéndez et al., 2011]. When matter is under such pressure the bonding distances decrease, inducing changes in all the properties of matter. The characterization of matter under high pressure is of interest by itself in fields as geophysics or astrophysics as the inherent conditions of matter inside the planets include high pressure. In addition, the gradual decrease of bonding distances changes the relative strengths of interactions in solids, so pressure is a powerful experimental tool to test physical models. Finally, high pressure induces phase transitions. Sometimes the high pressure polymorph can be recovered as a metastable phase, leading to a compound with advanced properties. Diamond and GaN are paradigmatic examples.

The determination of structural properties under high pressure is a prerequisite in high pressure studies. XAS is an invaluable tool in this task. In order to generate high pressures reasonable forces have to be applied to very small surfaces. The most widespread pressure cell is the diamond anvil cell (DAC) [Menéndez et al. 2011]. Sample dimensions vary from 10 to 100 microns, depending on the maximum pressure achieved. A μ-XAS beamline as the one proposed is well suited to perform high pressure XAS experiments. An example of one of these studies follows.

Titanate perovskites are technologically relevant materials with a rich phase diagram showing a strong competition between ferroelectric and antiferrodistorsive instabilities [Itié et al., 2010]. XRD depends on long range order and is thus sensitive to the TiO_6 rotations and distortions characteristic of the antiferrodistorsive instabilities. However, XRD averages the atomic arrangements over a large number of unit cells, and sometimes fails to provide clear information about the local structure. The experiment performed at LUCIA, the μ-XAS beamline in Soleil, clarifies the situation in $BaTiO_3$. At room pressure, $BaTiO_3$ is ferroelectric and crystallizes in a tetragonal structure. At 2 GPa a phase transition to a cubic structure is observed. Figure 16a shows the XANES spectra of BaTiO3 at the Ti K-edge. A large intensity of resonance B has been associated to the Ti off-center position. In Figure 16a resonance B decreases from ambient conditions to 10 GPa. The large intensity still observed after the phase transition indicates that Ti remains in off-center position in the cubic phase up to 10 GPa. In order to reconcile this fact with the cubic symmetry, the Ti off-center position must be disordered. XANES results have been correlated with the HP behavior of the diffuse reflectance observed in XRD images (Figure 16b), which is related to the pseudocubic symmetry and which disappears at 11 GPa [Ravi et al., 2007].

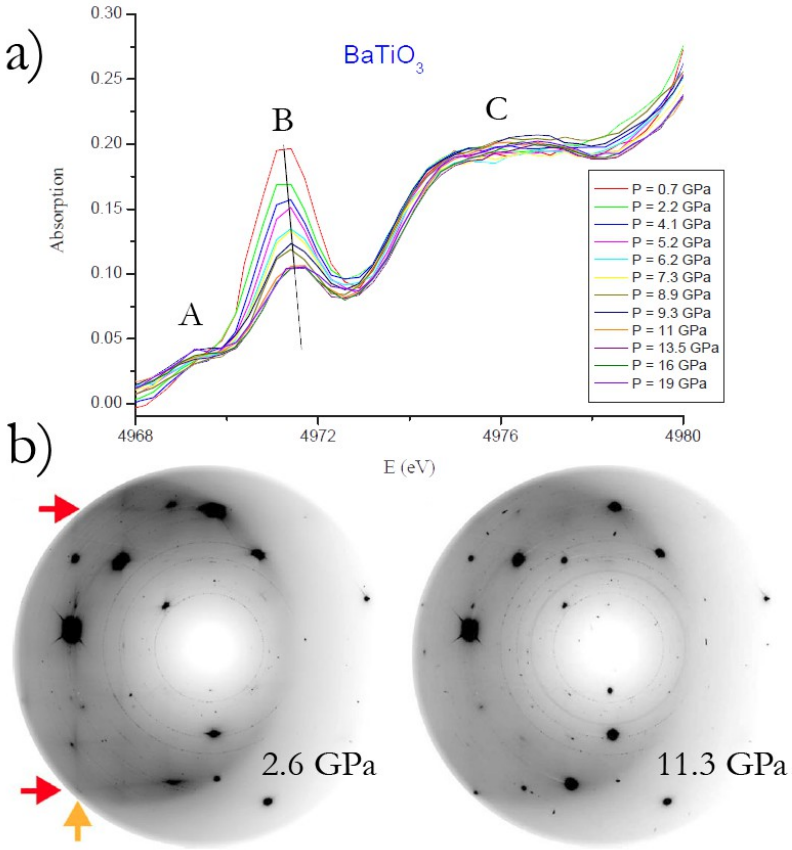

Figure 16: a) XANES spectra of BaTiO3 at the Ti K-edge. b) Selected XRD image plates.

Nanostructured SERS-based sensors

The fabrication of substrates for Surface Enhanced Raman Scattering (SERS) applications matching the needs for high sensitive and reproducible sensors remains a major scientific and technological issue. We correlate the morphological parameters of silver (Ag) nanostructured thin films prepared by sputter deposition on flat silicon (Si) substrates with their SERS activity. A maximum enhancement of the SERS signal has been found at the Ag percolation threshold, leading to the detection of thiophenol, a non-resonant Raman probe, at concentrations as low as 10^{-10} M, which corresponds to enhancement factors higher than 7 orders of magnitude. To gain full control over the developed nanostructure, we employed the combination of in-situ time-resolved microfocus Grazing Incidence Small Angle X-ray Scattering with sputter deposition. This enables to achieve a deepened understanding of the different growth regimes of Ag. Thereby an improved tailoring of the thin film nanostructure for SERS applications can be realized.

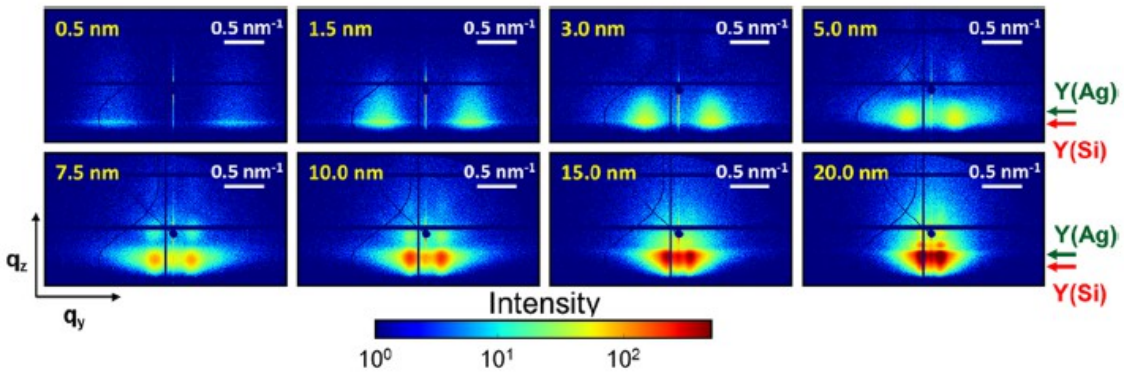

Figure 17: Selected 2D μGISAXS patterns during RF-sputter deposition of Ag. The corresponding effective film thickness is indicated in each image. The dark blue circle corresponds to the specular beam stop used to prevent the detector from being damaged due to the high X-ray intensity. The dark blue horizontal and vertical stripes correspond to the intermodule detector gaps. The positions of the Si Yoneda peak, Y(Si), and Ag Yoneda peak, Y(Ag), as well as the coordinate system (qy,qz) are indicated.

Conclusions

The richness in the diversity of materials properties occurs because of the countless combinations of admixture in chemical compositions, bonding types, crystal structures and morphologies. A review of the relationship among several of those aspects based on challenging subjects addressed by different research teams has been presented above. Solid state related issues dealt with by these teams include the use of chemical imaging for qualitative and quantitative analysis, the crystalline phases determined by XRD, the structural analysis using XANES/EXAFS, and furthermore the mesoscopic structure by SAXS/WAXS.

References

Chung H.-Y., Weinberger M. B., Levine J. B., Cumberland R. W., Kavner A., Yang J.-M., Tolbert S. H. and Kaner R. B., *Synthesis of ultra-incompressible superhard rhenium diboride at ambient pressure,* Science, 316, 436–9 (2007).

Flank A. M., Trcera N., Brunet F., Itié J. P., Irifune T., Lagarde P., *Experimental evidence of six-fold oxygen coordination for phosphorus and XANES calculations,* Journal of Physics: Conference Series 190 012174 (2009).

Gilliland, S., Segura, A., Sanchez-Royo J.F., Garcia L.M., Bartolome F., Sans J.A., Martinez-Criado G., Jimenez-Villacorta F., *Absence of ferromagnetism in single-phase wurtzite Zn1-xMnxO polycrystalline thin films,* J. Appl. Phys., 108, 073922(2010).

Gómez-Gómez M., et al. *Spontaneous core–shell elemental distribution in In-rich InGaN nanowires grown by molecular beam epitaxy.* Nanotechnology 25, 075705 (2014)

Itié J.P., Flank A. M., Lagarde P., Ravy S and Polian A., *High-pressure x-ray absorption spectroscopy: Application to the local aspects of phase transitions in ferroelectric perovskites*, in High-Pressure Crystallography: From Fundamental Phenomena to Technological Applications, Springer Science+Business Media B.V., 51-67 (2010).

Kawazoe H., Yasukawa M., Hyodo H., Kurita M., Yanagi H. and Hosono H., *p-type electrical conduction in transparent thin films of $CuAlO_2$*, Nature, 389, 939–42 (1997).

Martínez-Criado G., Somogyi A., Hermann M., Eickhoff M., Stutzmann M., *Direct Observation of Mn Clusters in GaN by X-Ray Scanning Microscopy*, Jpn. J. Appl. Phys. 43, L695 (2004).

Martínez-Criado G., Somogyi A., Tocoulou R., Salome M., Susini J., *Micro-XANES imaging for detecting metallic Mn in GaN*, Appl. Phys. Lett. 87, 061913, (2005).

Martínez-Criado G., Somogyi A., Ramos S., Campo J., Tocoulou R., Salome M., Susini J., Hermann M., Eickhoff M., Stutzmann M., Mn-*rich clusters in GaN: hexagonal or cubic symmetry?*, Appl. Phys. Lett. 86, 131927, (2005).

Martinez-Criado G., Segura A., Sans J.A., Homs A., Pellicer-Porres J., Susini, J., *X-ray absorption of $Zn_{1-x}Co_xO$ thin films: A local structure study*, Appl. Phys. Lett. 89, 061906 (2006).

Martínez-Criado, G. et al. *X-ray absorption in GaGdN: A study of local structure* Appl. Phys. Lett. 93, 021916 (2008)

Menéndez J. M., Aguado F., Valiente R. y Recio J. M., coordinadores, *Materia a alta presión. Fundamentos y aplicaciones*, Ediciones de la Universidad de Oviedo (2011).

Pellicer-Porres J, Segura A., Sánchez-Royo J. F., Sans J. A., Itié J. P, Flank A. M., Lagarde P. and Polian A., *Local environment of a diluted element under high pressure: $Zn_{1-x}Mn_xO$ probed by fluorescence x-ray absorption spectroscopy*, Appl. Phys. Lett., 89, 231904 (2006).

Pellicer-Porres J., Saitta A. M., Polian A., Itié J. P. and Hanfland, M., Six-fold-coordinated phosphorus by oxygen in $AlPO_4$ quartz homeotype under high pressure, Nat. Mat. 6, 698-702 (2007).

Pellicer-Porres J., Segura A., Muñoz A., Polian A. and Congeduti A., *Bond length compressibility in hard ReB_2 investigated by x-ray absorption under high pressure,* J. Phys.: Condens. Matter, 22, 045701 (2010).

Pellicer-Porres J., Segura A., Ferrer-Roca, Ch., Polian A., Munsch P. and Kim D., *XRD and XAS structural study of $CuAlO_2$ under high pressure*, J. Phys.: Condens. Matter, 25, 115406 (2013).

Ravy, S., Itié, J.P., Polian, A., and Hanfland, M., *High-pressure study of X-ray diffuse scattering in ferroelectric perovskites*, Phys. Rev. Lett., 99, 117601 (2007).

Sancho-Juan O., Cantarero A., Martínez-Criado G., Homs A., Garro N., Cros A., Dhar S., *XANES at the Mn K-edge in highly homogenous $Ga_{1-x}Mn_xN$ alloys*, Phys. stat. sol. (b) 243, 1692, (2006).

Sancho-Juan O., Cantarero A., Martínez-Criado G., Garro N., Cros A., Salome M., Susini J., Olguin D., Dhar S., *X-ray absorption near-edge structure of GaN with high Mn concentration grown on SiC*, J. Phys. Condens. Matt., 21, 295801 (2009).

Sancho-Juan O., Martínez-Criado G, Cantarero A., Garro N., Salomé M., Susini J., Olguín D, Dhar S., and Ploog K., *Extended x-ray absorption fine structure in $Ga_{1-x}Mn_xN$/SiC films with high Mn content*, Phys. Rev. B., 89, 172103 (2011).

Sans J. A., Martínez-Criado G., Pellicer-Porres J., Sánchez-Royo J. F., Segura A., *Thermal instability of electrically active centers in heavily Ga-doped ZnO thin films*, Appl. Phys. Lett. 91, 221904, (2007a).

Sans J. A., Sánchez-Royo J. F., Pellicer-Porres J., Segura A., Guillotel E., Martinez-Criado G., Susini J., Muñoz-Paez A., López-Flores V., *Optical, X-ray absorption and photoelectron spectroscopy investigation of the Co site configuration in Zn1-xCoxO films prepared by PLD*, Superlattices Micros. 42, 226, (2007b).

Sans J. A., Martinez-Criado G., Susini J., Sanz R., Jensen J., Minguez I., Hernandez-Velez M., Labrador A., Carpentier P., *Thermal instability of implanted Mn ions in ZnO*, J. Appl. Phys., 107, 023507 (2010).

G. Santoro, S. Yu, M. Schwartzkopf, P. Zhang, Sarathlal Koyiloth Vayalil, J. F. H. Risch, M. A. Rübhausen, M. Hernández, C. Domingo, S. V. Roth. Appl. Phys. Lett. 104, 243107 (2014).

Segura-Ruiz J, Martinez-Criado G, Chu MH, Geburt S, Ronning C, *Nano-X-ray Absorption Spectroscopy of Single Co-Implanted ZnO Nanowires*, Nano Lett. 11, 5322-5326 (2011).

Segura-Ruiz, J. et al. *Direct observation of elemental segregation in InGaN nanowires by X-ray nanoprobe.* Phys. Stat. Sol. RRL 5, 95-97 (2011)

Somogyi A., Martinez-Criado G., Homs A., Hernandez-Fenollosa M.A., Vantelon D. Ambacher O., *Formation of Si clusters in AlGaN:A study of local structure*, Appl. Phys. Lett. 90, 181129, (2007).

Materials science: soft condensed matter

Soft matter field is a relatively young sub-field of materials science generally described as the sort of materials that are easily deformed by mechanical stresses or thermal fluctuations. They include liquids, colloids, polymers, foams, gels, granular materials, liquid crystals, and a number of biological materials. Their study has a strong focus on understanding macromolecular assemblies, ussually from organic, but also frequently from inorganic origin. These meso-scale or medium sized constituents often self-assemble or organize into macro-scale materials and demonstrate many novel and unexpected phenomenon. Many of these materials are extremely familiar from everyday life and have a vast number of technologically important applications. In this field, the use of SAXS and WAXS is frequent due to the typical size of the long range order periods. Some application examples of synchrotron microprobes on heterogeneous and mesoscopic systems follows.

Confinement-induced phase transition in polymers

Ferroelectric polymers have emerged as cost-effective functional materials for organic electronic devices due to their high electric breakdown field, low dielectric loss, light weight and high flexibility. High aspect ratio (length/diameter) one-dimensional (1D) nanostructures are appropriate for studying size-dependent processes with length scales comparable to the nanostructure's size and may also have greater potential for high density energy storage applications due to the dramatically increased surface area over thin films and low aspect ratio nanostructures.

High aspect ratio 1D nanoarrays of poly(vinylidene fluoride) (PVDF) supported by a residual polymer film have been prepared by template wetting, using porous anodic aluminum oxide (AAO) as a template. X-ray microdiffraction (μ-XRD) experiments were carried out at ID13 (ESRF) to explore the heterogeneities along the 1D nanostructures in order to select the optimum parameters for improving the ferroelectric character of polymer nanoarrays. Scanning μ-XRD with a 1 μm diameter beam was accomplished along the cross-section of the samples with diffraction patterns collected at regular intervals between the residual PVDF film (bulk) and the nanowires. The information obtained from the wide-angle X-ray scattering (WAXS) is complementary to small-angle X-ray scattering (SAXS) due to the difference in length scales being probed.

This powerful tool reveals (Figure 18) the spatial evolution of the solid-solid phase transition from the α-nonpolar crystal form (bulk) to the γ-polar ferroelectric form (nanowires). It also allows the degree of crystallinity, and the crystal orientation to be investigated, providing information over multiple length scales simultaneously. [García-Gutiérrez et al. (2010 and 2013), ESRF highlights (2014)]

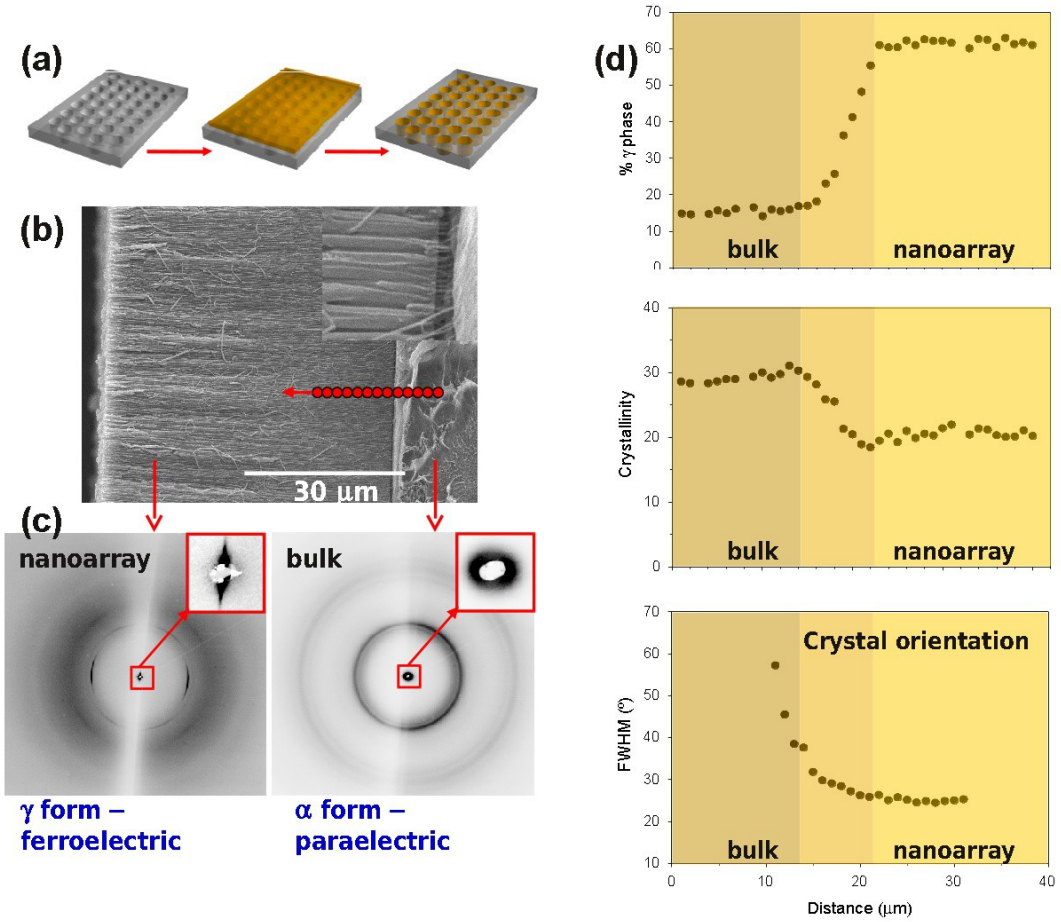

Figure 18: (a) The template wetting process to build the PVDF nanoarray. (b) SEM picture showing both the nanoarray and the bulk PVDF, and the points (in red) where the µ-XRD diagrams were taken. (c) SAXS/WAXS patterns taken at both the nanoarray and bulk zones of the sample, showing the nanoarray symmetry. (d) Phase ratio, crystallinity and crystal orientation results obtained from the µ-XRD diagrams taken at the points shown in (b)

Characterization of polymer superstructures

Radial symmetry is essential for the conventional view of the polymer spherulite microstructure. Typically it is assumed that, in the course of the spherulite morphogenesis, the lamellar crystals grow radially. Using submicron X-ray diffraction, it is shown that in banded spherulites of poly(propylene adipate) the crystals have the shape of a helix with flat-on crystals winding around a virtual cylinder of about 6 µm in diameter (Figure 19). The helix angle of 30° implies that the crystal growth direction is tilted away from the spherulite radius by this angle. The implications of the helical crystal shape contradict the paradigm of the spherulitic microstructure. The radial growth rate of such spherulites does not correspond to the crystal growth rate, but to the propagation rate of the virtual cylinder the ribbons wind around.

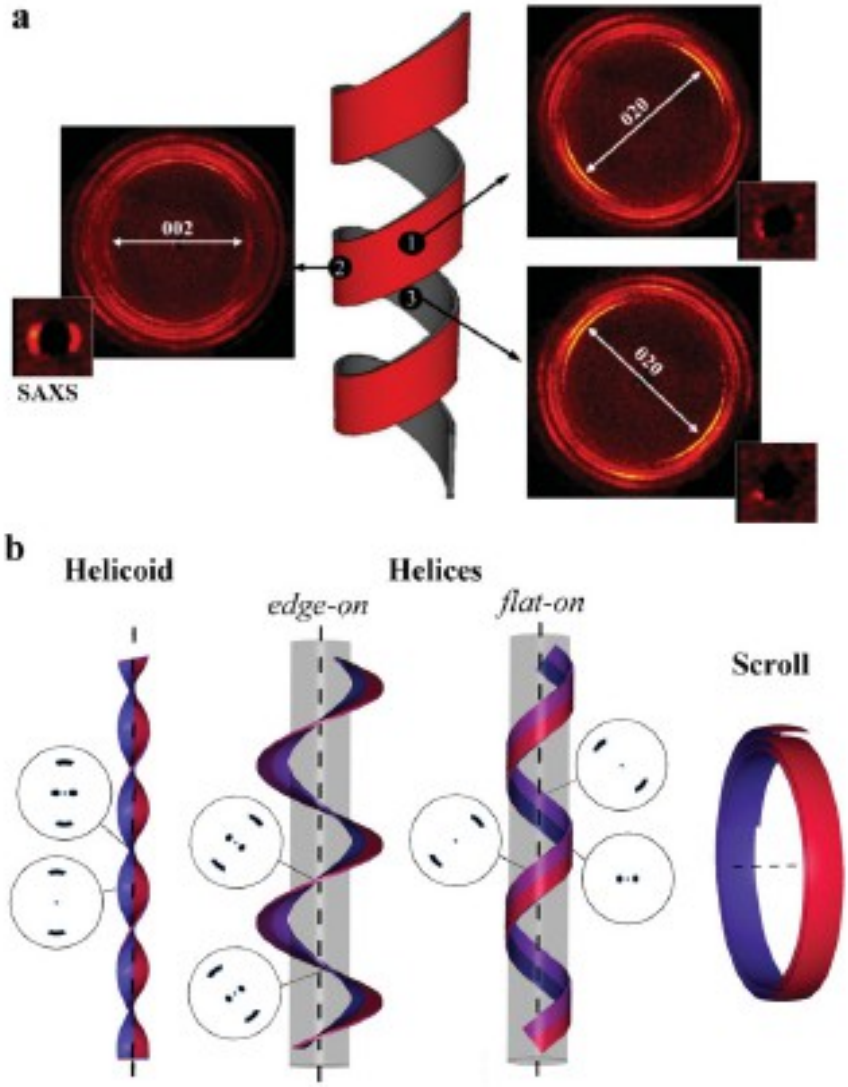

Figure 19: a) Experimental 2D X-ray submicron-diffraction patterns assigned to different positions along the helical crystalline lamella. b) Model of the classical helicoid, helices with edge-on and flat-on oriented lamella ribbon and a scroll together with the model nanofocus X-ray patterns corresponding to different spatial positions of the beam.

Segregation in hybrid organic-inorganic materials

Activated carbon fiber (ACF)/polyaniline (PANI) materials have been prepared using two different methods, viz. chemical and electrochemical polymerization. Electrochemical characterization of both materials shows that the electrodes with polyaniline have a higher capacitance than does a pristine porous carbon electrode. To analyze the distribution of PANI within the ACF, characterization by position-resolved microbeam small-angle X-ray scattering (μSAXS) has been carried out. μSAXS results obtained with a single ACF indicate that, for the experimental conditions used, a PANI coating is formed inside the micropores and that it is higher in the external regions of the ACF than in the core. Additionally, it seems that the penetration of PANI inside the fibers occurs in a larger extent for the chemical polymerization

or, in other words, for the electrochemically polymerized sample there is a slightly larger accumulation of PANI in the external regions of the ACF.

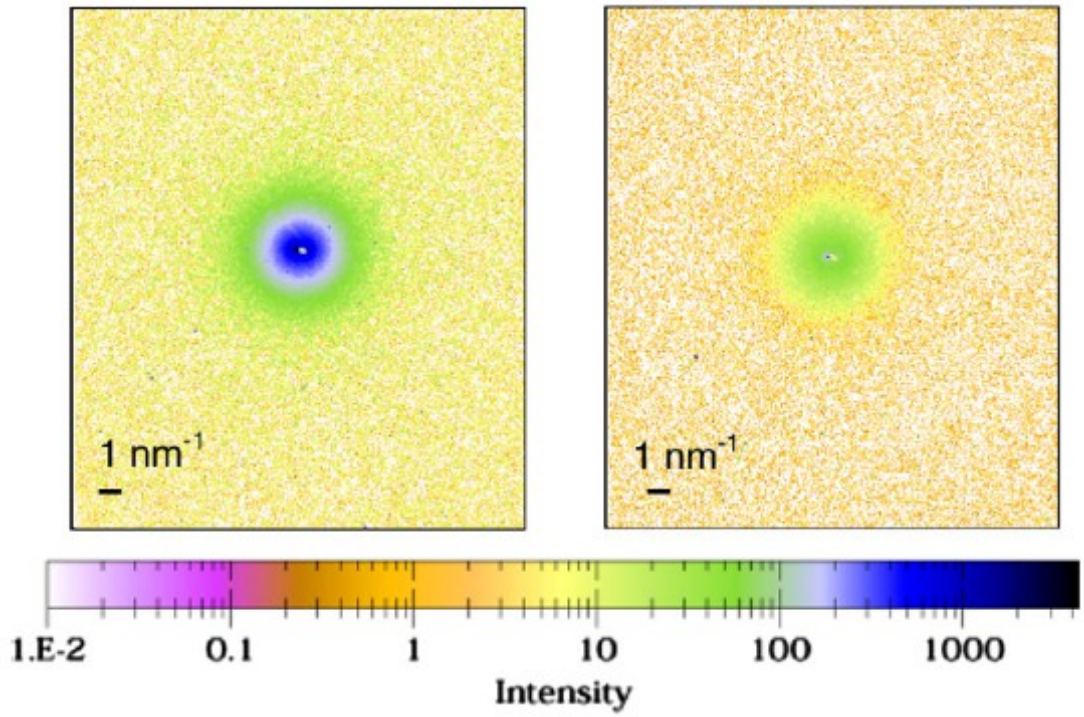

Figure 20: Two-dimensional scattering patterns obtained at the center of the fiber of the A20 sample (left) and the A20/PANI sample prepared using chemical polymerization method (A20_C) (right).

Conclusions

Soft condensed matter is a field with still a large ground to be studied. The varied characteristics of soft materials come not only from their composition and atomic structure, like hard systems, but also from their mesostructure. Beam sizes in the μm-range or less allow probing local heterogeneities, such as segregation in hybrid organic-inorganic materials [Salinas-Torres et al. (2012)], confinement effects in polymer nanostructures [García-Gutiérrez et al. (2010 and 2013), ESRF highlights (2014)] and templating of liquid crystals in nanopores [Pisula et al. (2006)]. The possibilities for in-situ studies during stretching, extrusion, or indentation have been proved [Riekel (2000)]. μ-SAXS/WAXS techniques can be used in a "bottom-up" or a "top-down" approach. Single-crystal diffraction corresponds to a "bottom-up" approach. The top-down approach corresponds to a local probing of functional material with a lateral resolution corresponding to the beam size. The experiments can be performed in situ on a whole sample, which also could correspond to in vivo conditions for a biological specimen. A μ-SAXS/WAXS mesh-scan provides a composite "diffraction image" of the material combining both real and reciprocal space information [Davies et al. (2007), Chanzy et al. (2006)], allowing elucidating the paradigm of polymer superstructures [Rosenthal et al. (2013)], as well as correlating the order and the orientation of the molecules of liquid crystals with physical properties and device performance [Kastler et al. (2006), Pisula et al. (2007)]. The multi-technique approach of the proposed beamline has been the key in these studies, by providing all the necessary tools at the same instrument.

References

ESRF Highlights 2013, 65 (2014).

Ralph Döhrmann, Stephan Botta, Adeline Buffet, Gonzalo Santoro, Kai Schlage, Matthias Schwartzkopf, Sebastian Bommel, Johannes F. H. Risch, Roman Mannweiler, Simon Brunner, Ezzeldin Metwalli, Peter Müller-Buschbaum, Stephan V. Roth. "A new highly automated sputter equipment for in situ investigation of deposition processes with synchrotron radiation". Rev. Sci. Instrum. 84, 043901 (2013).

K. M. O. Håkansson, A. B. Fall, F. Lundell, S. Yu, C. Krywka, Stephan V. Roth, Gonzalo Santoro, Mathias Kvick, Lisa Prahl Wittberg, Lars Wågberg, L. Daniel Söderberg. "Hydrodynamic alignment and assembly of nanofibrils resulting in strong cellulose filaments". Nature Comm. (2014). DOI: 10.1038/ncomms5018.

G. Herzog, G. Benecke, A. Buffet, B. Heidmann, J. Perlich, J. F. H. Risch, G. Santoro, M. Schwartzkopf, Shun Yu, Wilfried Wurth, Stephan V. Roth. "In Situ Grazing Incidence Small-Angle X-ray Scattering Investigation of Polystyrene Nanoparticle Spray Deposition onto Silicon". Langmuir, 29, 11260−11266 (2013).

M. Kastler, W. Pisula, F. Laquai, A. Kumar, R.J. Davies, S. Baluschev, M.C García Gutiérrez, D. Wasserfallen, H.J. Butt, C. Riekel, G. Wegner, K. Müllen. "Organisation of charge-carrier pathways for organic electronics". Advanced Materials 18, 2255-2259 (2006).

V. Korstgens, M. Philipp, D. Magerl, M. A. Niedermeier, G. Santoro, S. V. Roth, P. Müller-Buschbaum. "Following initial changes in nanoparticle films under laminar flow conditions with in situ GISAXS microfluidics" RSC Adv., 4, 1476–1479 (2014).

M.C. García Gutiérrez, J. Karger-Kocsis, C. Riekel."Cold drawing-induced mesophase in amorphous poly(ethylene naphthalate) revealed by X-ray microdiffraction". Macromolecules 35, 7320-7325 (2002).

M.C. García-Gutiérrez, A. Nogales, D.R. Rueda, C. Domingo, J.V. García-Ramos, G. Broza, Z. Roslaniec, K. Schulte, R. J. Davies, T. A. Ezquerra."Templating of crystallization and shear-induced self-assembly of single-wall carbon nanotubes in a polymer-nanocomposite" Polymer 47, 341-345 (2006).

M.C. García Gutiérrez, G.C. Alfonso, C. Riekel, F. Azzurri."Spatially resolved flow-induced crystallization precursors in isotacti polystyrene by simultaneous small- and wide- angle X-ray microdiffraction". Macromolecules 37, 478-485 (2004).

M.C. García Gutiérrez, A. Gourrier, C. Riekel."Investigation of Structural Processes during Indentation of Polymers by Synchrotron Radiation Microdiffraction". Journal of Macromolecular Science, Physics 43, 267-277 (2004).

M.C. García-Gutiérrez, A. Nogales, D.R. Rueda, C. Domingo, J.V. García-Ramos, G. Broza, Z. Roslaniec, K. Schulte, T. A. Ezquerra. "X-ray Microdiffraction and Micro-Raman study on an injection moulding SWCNT-polymer nanocomposite". Composites Science and Technology 67, (2007).

García-Gutiérrez, M.C., Linares, A., Hernández, J.J., Rueda D.R., Ezquerra, T.A., Poza, P., Davies, R.J.. Nano Letters 10, 1472 (2010).

García-Gutiérrez, M.C., Linares, A., Martín-Fabiani, I., Hernández, J.J., Soccio, M., Rueda, D.R., Ezquerra, T.A., Reynolds, M., Nanoscale 5, 6006 (2013).

M.C. García-Gutiérrez, A. Linares, I. Martín-Fabiani, J.J. Hernández, M. Soccio, D.R. Rueda, T.A. Ezquerra, M. Reynolds. "Understanding crystallization features of P(VDF-TrFE) copolymers under confinement to optimize ferroelectricity in nanostructures". Nanoscale, 5 (13) 6006-6012 (2013).

Mari-Cruz García-Gutiérrez, Amelia Linares, Jaime J. Hernández, Daniel R. Rueda, Tiberio A. Ezquerra, "Confinement-Induced One-Dimensional Ferroelectric Polymer Arrays". Pedro Poza and Richard J. Davies. Nanoletters 10(4), 1472–1476 (2010).

A. Gourrier, M.C. García Gutiérrez, C. Riekel. "Combined Microindentation and Synchrotron Radiation Microdiffraction applied to Polymers". Macromolecules 35, 8072-8077 (2002).

A. Gourrier, M.C. García Gutiérrez, C. Riekel. "Hardness Testing Under a Different Light: Combining Synchrotron X-Ray Microdiffraction and Indentation Techniques for Polymer Fiber Structure". Philosophical Magazine 86, 5753-5767 (2006).

A. Gourrier, M.C. García Gutiérrez, C. Riekel. "Investigation of the Structural Deformation Mechanisms induced by Microindentation in a Thermotropic Liquid Crystalline Copolyester using Synchrotron X-ray

Microdiffraction". Macromolecules 38, 3838-3844 (2005).

Lozano-Castello D, Cazorla-Amoros D., Linares-Solano A. "Microporous solid characterization: Use of classical and "new" techniques".Chemical Engineering Technology, 26, 852-857(2003).

Lozano-Castelló D, Raymundo Piñero E, Cazorla- Amoros D, Linares-Solano A, Müller M, Riekel C. "Microbeam SAXS: A novel technique for the characterization of activated carbon fibers". Studies in surface science and catalysis; COPS, 144, 51-58, (2002), Elsevier.

Lozano-Castelló D, Raymundo-Piñero E, Cazorla-Amoros D, Linares-Solano A. Müller M, Riekel C. "Characterization of pore distribution in activated carbon fibers by microbeam small angle X-Ray scattering". Carbon, 40: 2727-2735 (2002).

Maciá-Agulló J.A., Lozano-Castello D., Cazorla-Amorós D., Linares-Solano A., Müller M., Burghammer M., Riekel C., "Simultaneous tensile stress and microbeam small angle X-ray scattering (micro-SAXS) measurements on single activated carbon fibres". Carbon 2004, July 2004, Brown University, USA.

I. Martín-Fabiani, M.C. García-Gutiérrez, D.R. Rueda, A. Linares, J.J. Hernández, T.A. Ezquerra, M. Reynolds. "Crystallization under one-dimensional confinement in alumina nanopores of Poly (trimethylene terephthalate) and its composites with Single Wall Carbon Nanotubes". ACS Appl. Mater. Interfaces, 5 (11) 5324-5329 (2013).

W. Pisula, M. Kastler, B. El Hamahoui, M.C. García-Gutiérrez, R.J. Davies, C. Riekel, K. Müllen. "Dendritic morphology in homeotropically aligned hexa-peri hexabenzocoronene films". ChemPhysChem, 8, 1025 (2007).

W. Pisula, M. Kastler, D. Wasserfallen, M.C García-Gutiérrez, K. Müllen. "From Macro- to Nanoscopic Templating with Nanographenes". Journal of the American Chemical Society 128, 14424-14425 (2006).

M. Rosenthal, J.J. Hernández, Y.I. Odarchenko, M. Soccio, N. Lotti, E. Di Cola, M. Burghammer, D. A. Ivanov. Macromol. Rapid Commun. 34, (23-24), 1815-1819 (2013).

M. Rosenthal , J. J. Hernandez , Y. I. Odarchenko , M. Soccio , N. Lotti , E. Di Cola , M. Burghammer , D. A. Ivanov. "Non-Radial Growth of Helical Homopolymer Crystals: Breaking the Paradigm of the Polymer Spherulite Microstructure" Macromol. Rapid Commun, 34, (23-24), 1815-1819 (2013).

M. Rosenthal, D. Doblas, J. J. Hernandez, Y. I. Odarchenko, M. Burghammer, E. Di Cola, D. Spitzer, A. E. Antipov, L. S. Aldoshina, D. A. Ivanov. "High-resolution thermal imaging with a combination of nano-focus X-ray diffraction and ultra-fast chip calorimetry" J. Synchrotron Rad., 21, 223–228 (2014).

C. Riekel, M.C. García Gutiérrez, A. Gourrier, S. Roth."Recent synchrotron radiation microdiffraction experiments on polymer and biopolymer fibres". Analytical and Bioanalytical Chemistry 376, 594-601 (2003).

D. Salinas-Torres; J.M. Sieben; D. Lozano-Castello; E. Morallon; M.Burghammer; C. Riekel; D. Cazorla-Amoros "Characterization of activated carbon fiber/polyaniline materials by position-resolved microbeam small-angle x-ray scattering" Carbon 50 (2012) 1051-1056.

G. Santoro, S. Yu, M. Schwartzkopf, P. Zhang, Sarathlal Koyiloth Vayalil, J. F. H. Risch, M. A. Rubhausen, M. Hernández, C. Domingo, S. V. Roth. "Silver substrates for surface enhanced Raman scattering: Correlation between nanostructure and Raman scattering enhancement". Appl. Phys. Lett. 104, 243107 (2014).

G. Santoro, S. Yu, C. Krywka, S. V. Roth, G. Ellis. "Microfocus X-ray scattering and micro-Raman spectroscopy: Transcrystallinity in isotactic polypropylene". Phys. St. Sol. (2014) doi: 10.1002/pssr.201409207.

D. Sen, J. Bahadur, S. Mazumder, G. Santoro, S. Yub, S. V. Roth. "Probing evaporation induced assembly across a drying colloidal droplet using in situ small-angle X-ray scattering at the synchrotron source" Soft Matter, 10, 1621–1627 (2014).

Torre, J; Cortazar, M; Gomez, MA; Marco, C; Ellis, G; Riekel, C; Dumas, P. "Nature of the crystalline interphase in sheared iPP/vectra fiber model composites by microfocus X-ray diffraction and IR microspectroscopy using synchrotron radiation" Macromolecules, 39, 5564-5568 (2006).

S. Yu, G. Santoro, K. Sarkar, B. Dicke, P. Wessels, S. Bommel, R. Döhrmann, J. Perlich, M. Kuhlmann, E. Metwalli, J. F. H. Risch, M. Schwartzkopf, M. Drescher, P. Müller-Buschbaum, S. V. Roth. "Formation of Al Nanostructures on Alq3: An in Situ Grazing Incidence Small Angle X-ray Scattering Study during Radio Frequency Sputter Deposition" J. Phys. Chem. Lett., 4, 3170−3175 (2013).

Biomedical and bioenvironmental science

Over the last years, the role played by synchrotron based microprobes has been increasing in life sciences. Trace element imaging and speciation analysis in cells and subcellular compartments have been undertaken to better understand the biological chemistry of essential or toxic elements. The knowledge of intracellular distribution of chemical elements is a key target in the comprehension of biological processes occurring within cells. A cell contains about twenty different chemical elements, which are handled in a quite specific fashion. Although biological organisms are mainly constituted of organic matter (H, C, N, O) and mineral elements (Na, Mg, Si, P, S, Cl, K, Ca), many regulation systems and intracellular processes are subordinated to the presence or lack of one or more given elements, mainly metals (Mn, Fe, Co, Cu, Zn, Mo, Se, I) at trace concentration levels. Anomalous spread of essential elements can lead to cellular dysfunction. The toxicity of hazardous elements (Cr, As, Cd, Ba, heavy metals) also depends on their ability to reach specific intracellular targets such as the nucleus or the mitochondria. In-situ analyses of those elements within cells require the use of analytical probes that can achieve both high spatial resolution in the micrometer range and very low detection limits. The quantitative capability of micro-analytical techniques is also an essential characteristic as metal toxicity is strongly correlated to concentration.

So far various studies have been undertaken dealing with tissues, plants, some micro-organisms and animals, or human cells. By simultaneous elemental and chemical mapping, the synchrotron based microprobes have provided: 1) a better understanding of diseases and immune processes, as well as toxin and heavy metal uptake down to a micron cellular level; 2) a better insight of the functionality of a large number of metallo-proteins through the study of the spatial distribution and chemical properties of such species in cells and tissues; 3) a mapping of the distribution and biotransformations of anti-cancer and other drugs in cultured cells and tissues in order to gain a better idea of drug pharmacology and pharmacokinetics for improved drug design and delivery; 4) two-dimensional scanning of chromatography gels in which all of the proteins of an organism or an organ are separated; 5) XANES and EXAFS can be used to determine the local environment about the absorbing atom(s) in order to identify the type of metallo-protein or the sulfur donors in a protein; 6) a better understanding of the distribution, uptake and metabolism of metal-containing pharmaceutics in cells and tissue for the development of better and safer drugs. μ-XAS can provide structural chemical information regarding the intracellular biotransformation of the drugs; 7) gene maps obtained by attaching different metal oxides to DNA and RNA sequences and scanning them by a sub-micron X-ray beam. The following section describes some of these biomedical and bioenvironmental applications.

Drug and oligoelements mapping in cancer research

Reports in the literature indicate a superior effectiveness of anticancer treatments using drugs liposome-encapsulated. In this recent work [Gil, et al., 2014], the influence of the drug cisplatin associated with lipid vesicles (liposomes) is studied. Possible induced changes in the elemental composition, distribution, and concentration inside F98 glioma cells are investigated by synchrotron X-ray fluorescence (XRF). XRF at nanometer spatial resolution provides information on the two-dimension variation of elements inside the cells.

After the drug was administered, surviving and dead cells were studied. Figure 21 shows the XRF mapping of a liposome from a surviving cell, with the different elements studied.

These range from the Pt associated to the cisplatin drug, to the oligoelements Ca, K and Zn.

In comparison with dead cells, the elemental analysis shows that both platinum and zinc contents decrease in surviving samples. Moreover, higher levels of calcium and lower levels of potassium are revealed in dead cells, especially in those treated with liposomal cisplatin. These findings would mean that liposome-treated cells died mainly by apoptosis (programmed, non traumatic death). Although further analyses are still necessary, the results presented in this work suggest that the lipid vesicles could provide, thus, a methodology for an effective platinum administration.

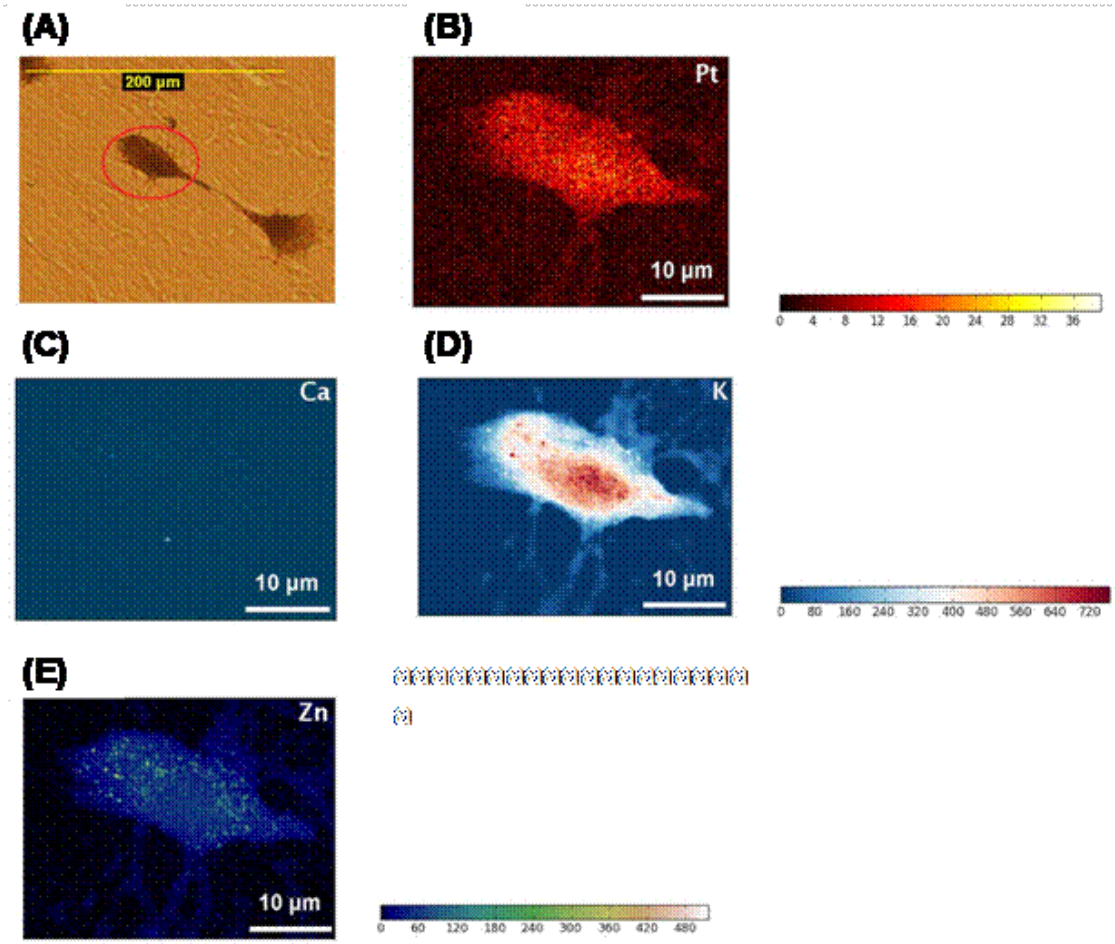

Figure 21: (a) Microscopy image of the studied liposome from a surviving cell after the cisplatin treatment. (b) Pt, (c) Ca, (d) K, and (e) Zn µ-XRF mapping diagrams, showing the oligoelement content in the liposome, in ppm.

Oligoelement content related to Parkinson's disease

Neurodegenerative cascades in Parkinson's disease (PD) involve protein aggregation and oxidative stress, although the triggers for these events are unknown. Changes in biometals have long been suspected to play a role in these cascades. Cu is an important biometal in the brain, and significant decrease in total tissue Cu in the degenerating substantia nigra in PD has been consistently reported over a number of decades and recent evidence suggests that

peripheral Cu metabolism is also altered. The complexing of Cu with the PD-associated protein k-synuclein increases aggregation and toxicity of this protein, possibly via stimulation of free radical production. On the other hand, Cu is also a critical cofactor in a range of cuproproteins, including the key protective cellular antioxidant superoxide dismutase 1 (SOD1). Studies in model systems demonstrate that Cu depletion is associated with reduced activity of SOD1 and a concomitant increase in free radical production, which can be normalized by Cu supplementation. SOD1 activity is reduced in the plasma of PD patients and studies in animal models of PD suggest that overexpression of SOD1 increases neuronal survival. These data suggest that a reduction in brain Cu in PD may reduce SOD1-mediated antioxidant defense and contribute to neurodegenerative cascades. In this work [Davies et al., 2014], changes in neuronal Cu levels and transport pathways are investigated to determine if changes in Cu are associated with a reduced antioxidant capacity in regions of neurodegeneration in PD.

Cu levels were quantified within single neurons as well as regions in thin sections (20 µm) cut from fixed or frozen tissue samples using synchrotron radiation X-ray fluorescence microscopy (XFM) using a microprobe beam, with a step size of 1 µm.

Quantitative analysis of fixed sections by XFM (Figure 22) revealed a 45% decrease in associated Cu in the substantia nigra from PD cases with respect to both age-matched controls. Furthermore, Cu levels were unchanged in regions that do not degenerate in PD, so it appears that this early decrease is specific to regions vulnerable to neuronal cell loss in this disorder.

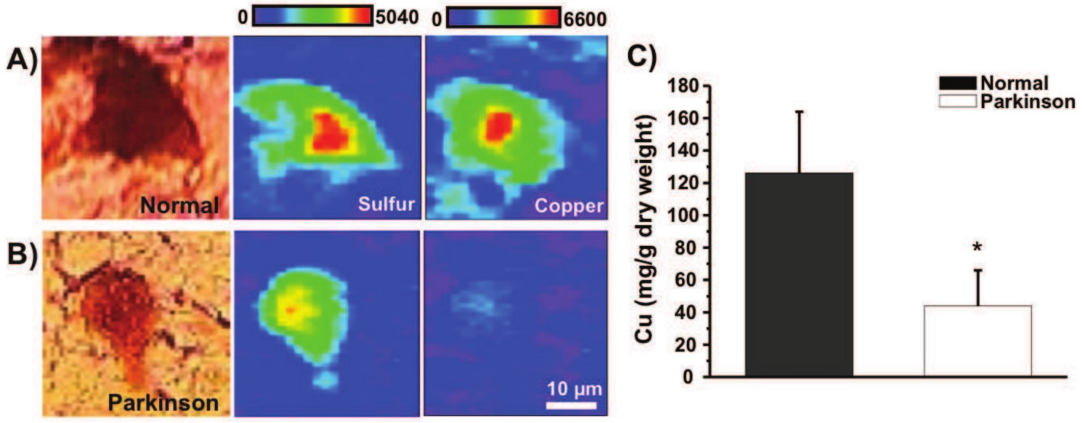

Figure 22: Microscopy and XRF mapping of S and Cu of a healthy (a) and Parkinson's affected (b) neurone. (c) Quantification of the Cu amount in the healthy and Parkinson's neurone

Toxic element acummulation in plants

Aluminum (Al) is a ubiquitous element without a known, specific, biological function. As one of the most abundant elements in the Earth crust, after Si and O, it is present in the daily life of all organisms. Al generally occurs as a component of a variety of crystalline minerals, and it is thus usually regarded as not being available for chemical and biological reactions. However, under acidic conditions (pH < 4.5), Al is solubilised into a toxic trivalent cation, Al^{3+}, which is more available for biochemical processes. Al^{3+} has a high affinity for O_2-donor compounds, and even the very low concentrations of free Al^{3+} in the symplasm are potentially

toxic. Indeed, micromolar concentrations of Al^{3+} can affect root growth and development in many agriculturally important plant species, and Al toxicity has been recognized as a major factor that limits plant performance in acidic soils. Nevertheless, some plants have adapted to this high Al^{3+} availability in acidic soils, especially in tropical regions, by developing resistance or tolerance mechanisms.

Among Al accumulators, the tea plant (Camellia sinensis (L.) O. Kuntze, Theaceae) is the subject of intense research. Studies of the localization and speciation of Al in tea leaves aim to provide a better understanding not only of Al-tolerance mechanisms in plants, but also of the fates and risks of dietary Al intake in humans who consume tea based beverages.

The aim of the present study [Tolrà et al., 2011] was to investigate the spatial distribution of Al and other low-Z elements in optimally developed leaves of tea plant using low-energy X ray fluorescence spectro-microscopy, after being grown on a controlled Al^{3+} enriched soil.

Localization of the elements in these tea-leaf cross sections using XRF showed that Al was mainly localized in the cell walls of the epidermal cells, as shown in Figure 23. The intense Al localization in these cell walls of epidermal cells confirms that Al is mainly moved through the leaf apoplastically, together with the water mass flow from the xylem to the epidermis, where the water then evaporates into the air and Al is concentrated in the cell walls at the sites of evaporation.

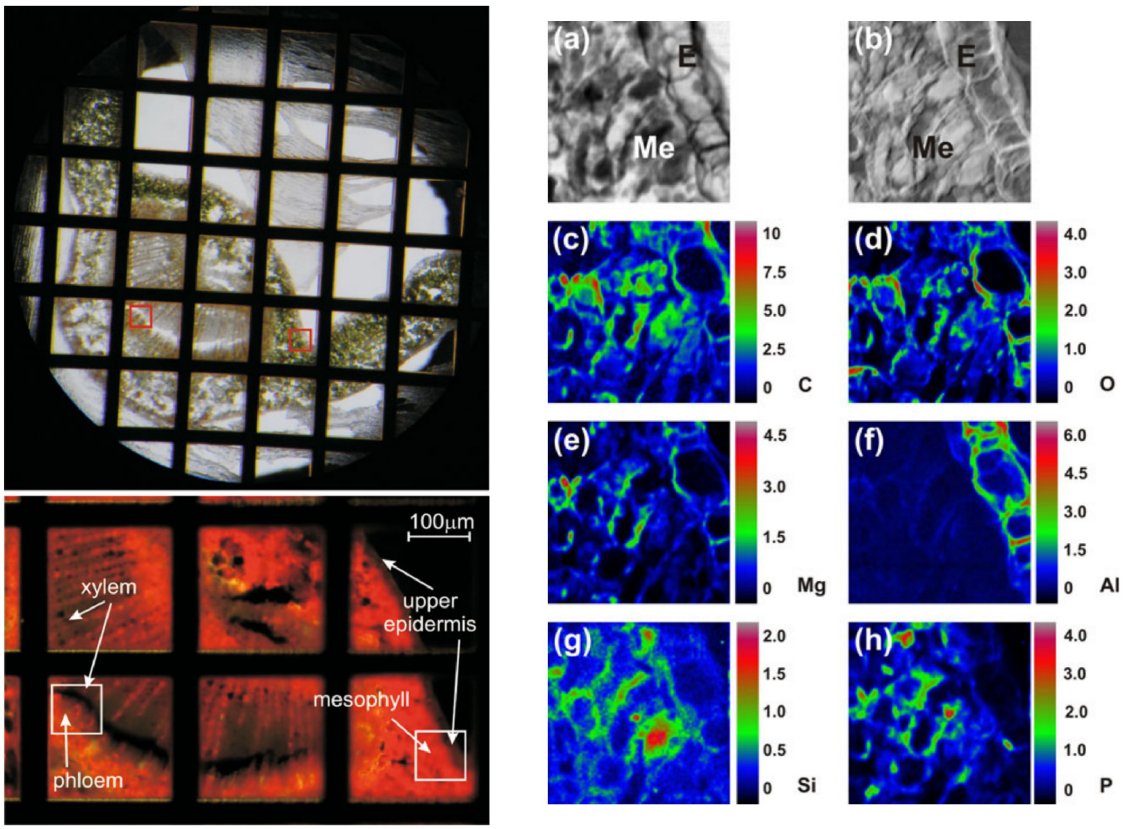

Figure 23: (left) Tea-plant leaf cross-section (20 µm thick) photographed under light stereo-microscope (left upper) and light microscope using blue light excitation source (left lower) with the indicated scanned regions of the epidermis–mesophyll and xylem–phloem. The size of the scanned regions was 80 x 80 µm2. (right) Scan of the representative epidermis–mesophyll region of a tea leaf (size 80 x 80 µm2, scan 80 x 80 pixels). (a) Bright field (absorption) image; (b) differential phase-contrast image; XRF maps of (c) C; (d) O; (e) Mg; (f)Al; (g) Si; and (h) P.

Conclusions

Life sciences is a relatively recent field within the synchrotron radiation community for various reasons, including the small sizes of samples, and the related difficulty to find the relevant spot to study, the usual low concentration of the studied elements and the frequent radiation damage. These makes a microfocus beamline specially suitable for this kind of systems, and would be of even greater interest if X-ray fluorescence tomography is available in a future development, to be capable of record 3D, element-resolved maps of the samples.

References

Curis E., Nicolis I., Bohic S., Somogyi A., Simionovici A., Bénazeth S., *Methodological study using XAS of an arsenic-based antileukemia treatment*, Physica Scripta,T115, 870-872, (2005).

Davies K.M., et al. *Copper pathology in vulnerable brain regions in Parkinson's disease.* Neurobiol. Aging 35(4) 858-66 (2014)

Eichert D., Salomé M., Banu M., Susini J., and Rey C., *Preliminary characterization of calcium chemical environment in apatitic and non-apatitic calcium phosphates of biological interest by X-ray absorption spectroscopy*, Spectrochimica Acta B, 60, 850-858 (2005).

Eichert D., Salomé M., Bleuet P., Bohic S., and Susini J., *Contribution of X-ray microscopy to bone mineral studies*, XRM 2005, Egret Himeji, Japon, in Procs. 8th Int. Conf. X-ray microscopy, IPAP conf. Series, 7, 210-212, (2006).

Eichert D, Gregoratti L, Kaulich B, Marcello A, Melpignano P, Quaroni L, Kiskinova M, *Imaging with spectroscopic micro-analysis using synchrotron radiation*, Analytical and Bioanalytical Chemistry, 389, 1121-1132, (2007).

Gil S., Carmona A., Martínez-Criado G., León A., Prezado Y., Sabés M. *Analysis of Platinum and Trace Metals in Treated Glioma Rat Cells by X-Ray Fluorescence Emission* Biological Trace Element Research DOI: 10.1007/s12011-014-0097-2 (2014)

Isaure MP, Fayard B, Saffet G, Pairis S, Bourguignon J, *Localization and chemical forms of cadmium in plant samples by combining analytical electron microscopy and X-ray spectromicroscopy*, Spectrochimica Acta B, 61, 1242-1252, (2006).

Isaure MP, Fraysse A, Deves G, Le Lay P, Fayard B, Susini J, Bourguignon J, Ortega R, *Micro-chemical imaging of cesium distribution in Arabidopsis thaliana plant and its interaction with potassium and essential trace elements*, Biochimie, 88, 1583-1590, (2006).

Moger C. J., Barrett R., Bleuet P., Bradley D. A., Ellis R. E., Green E. M., Knapp K.M., Muthuvelu P., Winlove C. P., *Regional Patterns of Collagen Orientation in Normal Articular Cartilage and Subchondral Bone and in Lesions of the Equine Metacorpophalangeal Joint Determined using X-ray Diffraction*, Osteoarthritis and Cartilage, (2006).

Ortega R., Devès G., Bohic S., Simionovici A., Ménez B., Bonnin-Mosbah M., *Iron Distribution in Cancer Cells Following Doxorubicin Exposure using Proton and X-ray Synchrotron Radiation Microprobes*, Nucl. Instr. Res. and Meth. B., 181, 480-84, (2001).

Ortega R., Devès G., Fayard B., Salomé M. , Susini J., *Combination of synchrotron radiation X-ray microprobe and nuclear microprobe for chromium and chromium oxidation states quantitative mapping in single cells* Nuclear Instruments and Methods in Physics Research, B 210,325-329, (2003).

Ortega R., Suda A., Devès G. *Nuclear microprobe imaging of gallium nitrate in cancer cells*. Nuclear Instruments and Methods in Physics Research B, 210, 364-367, (2003).

Ortega R., Bohic S., Tucoulou R., Somogyi A., Devès G., *Micro-chemical element imaging of yeast and human cells using synchrotron X-ray microprobe with Kirkpatrick-Baez optics*, Analytical chemistry, 76, 309-314, (2004).

Ortega R., Fayard B., Salomé M., Devès G., Susini J., *Chromium oxidation state imaging in mammalian cells exposed in vitro to soluble or particulate chromate compounds*, Chemical Research in Toxicology, 18,1512-

1519, (2005).

Ortega R., Fayard B., Salomé M., Devès G., Susini J., *Chromium oxidation state mapping in human cells*, Journal de Physique IV, 104, 289-292, (2003).

Oste L, Verberckmoes SC, Behets GJ, Dams G, Bervoets AR, Van Hoof VO, Bohic S, Drakopoulos M, De Broe ME, D'Haese PC, *Strontium incorporates at sites critical for bone mineralization in rats with renal failure*, X-Ray spectrometry, 71, 298-303 (2007).

Sarret G, Isaure MP, Marcus MA, Harada E, Choi YE, Pairis S, Fakra S, Manceau A, *Chemical forms of calcium in Ca,Zn- and Ca,Cd-containing grains excreted by tobacco trichomes*, Canadian Journal of Chemistry, 85, 738-746, (2007).

Szczerbowska-Boruchowska M., Lankosz M., Adamek D., Ostachowicz J., Krygowska-Wajs A., Szczudlik A., Bohic S., Simionovici A., Chwiej J., *Determination of trace elements in Parkinson's diseased brain tissue using microbeam of synchrotron radiation*, Journal Of Neurochemistry, 85, 23-24, (2003).

Szczerbowska-Boruchowska M. Lankosz M., Ostachowicz J., Adamek D., Krygowska-Wajs A., Tomik B., Szczudlik A., Simionovici A., Bohic S., *Topographic and quantitative microanalysis of human central nervous system tissue using synchrotron radiation*, X-Ray Spectrometry, 33(1), 3-11, (2004).

Szczerbowska-Boruchowska M., Chwiej J., Lankosz M., Adamek D., Wojcik S., Krygowska-Wajs A., Tomik B., Bohic S., Susini J., Simionovici A., Dumas P., Kastyak M., *Intraneuronal investigations of organic components and trace elements with the use of synchrotron radiation*, X-Ray Spectrometry, 34(6),514-520, (2005).

Tolrà R., et al. *Localization of aluminium in tea (Camellia sinensis) leave using low energy X-ray fluorescence spectro-microscopy.* J. Plant. Res. 124, 165–172 (2011)

Verberckmoes S.C., Behets G.J., Oste L., Bervoets A.R., Lamberts L.V., Drakopoulos M., Somogyi A., Cool P., Dorriné W., De Broe M.E., D'Haese P.C., *Effects of strontium on the physicochemical characteristics of hydroxyapatite*, Calcified Tissue International 75, 405-415.

Verberckmoes S.C., De Broe M.E., D'Haese P.C., *Dose-dependent effects of strontium on osteoblast function and mineralization*, Kidney International, 64, 534-543, (2003).

Behets G.J.,Verberckmoes S.C.,Oste L.,Bervoets A.R.,Salomé M.,Cox A.G.,Denton J.,De Broe M.E.,D'Haese P.C., *Localization of lanthanum in bone of chronic renal failure rats after oral dosing with lanthanum carbonate*, Kidney International, 67, 1830-1836 (2005).

Verberckmoes S.C., Persy V., Behets G.J., Neven E., Hufkens A., Hong Zebger-Gong, Müller D., Haffner D., Querfeld U., Bohic S., De Broe M.E., D'Haese P.C., *Uremia-related vascular calcification: More than apatite deposition*, Kidney International, 71, 298-303 (2007).

Design and budget

Strategic considerations

This project is guided by two current trends: first, the increasing strength of the hard X-ray microprobes, centred on the focusing optics quality, high setup flexibility and an unparalleled service to a broad user community. Second, the beamline proposal takes into account the current and new hard X-ray microprobes in Europe and elsewhere, matching the specific scientific demands of the Spanish user community and also complementing the present and future European X-ray microstations (e.g., ID21, and the new ID16A/B at ESRF, Nanoscopium and LUCIA at SOLEIL, Microprobe at PETRA III).

A large number of microprobes are available today, while several advanced projects are in the planning or realization phase. Figure 1 indicates most of the X-ray microprobes currently operational or planned at synchrotron radiation sources across the world.

In the soft X-ray regime, several high performance second-generation based microscopes have been operating for a number of years. Notable amongst these are those at ALS, ELETTRA and BESSY, all of which have made very significant scientific advances in X-ray microscopy. The intensity of these soft X-ray sources, coupled with innovative photon and electron optics, has opened the path to new, non-destructive, chemical species and magnetic atom selective microscopies. In addition to MISTRAL, the X-ray microscopy beamline at ALBA dedicated to transmission full-field imaging of biological thick samples from 270 eV to 2600 eV at cryo-temperatures, recent third-generation low energy sources (SLS, SOLEIL, BESSY II) have also given financial support for microscale imaging facilities using Fresnel zone plates. In the same way, in the hard X-ray regime all analytical techniques are also following the natural trend of pushing down the spatial resolution. Considering the dedicated microprobes in Europe (SLS, DIAMOND, SOLEIL), a very competitive context can be anticipated coming from the medium-energy synchrotron sources. The restricted access to synchrotron facilities has always been a limitation compared to electron microscopy or advanced light microscopy hampering a broader usage of X-ray microscopy and analysis. It can therefore be foreseen that the availability of an increased number of microprobes will actually lead to a wider usage of X-ray analytical imaging methods and the involvement of new user communities. The present project will allow ALBA to extend and offer the state-of-the-art in this context. Its success crucially depends on optimum performance of the ALBA source: lowest possible emittance, high spectral brightness (cryo-cooled in-vacuum undulator) and ultimate source stability of a storage ring. The latter requirement makes future sources such as X-FELs less appropriate to this field. Improved performance and improved accessibility are of crucial importance to the Spanish user communities.

Required techniques

XRF chemical mapping within sub-micron range (~ 0.5 x 0.5 μm^2). An extremely high spatial resolution is not required, but detection limits for concentration should be kept as low as possible mainly for environmental sciences. Differences in elemental distribution are generally indicative of different chemical states and compounds in the sample. The μ-XRF combined with mapping capabilities allows detecting and plotting the 2D distribution of the fluorescence lines of selected elements. The elemental distribution can be used in parallel to define regions of interest (ROI) during μ-XRD and μ-XANES/EXAFS experiments on

heterogeneous samples. The elemental detection limits on third generation synchrotrons with the appropriate focusing optics to maximize the photon flux can be lowered down to ppb. For μ-XRF the experimental set up is in fluorescence geometry with the sample sitting on a stage able to perform movements along XYZ axes at micron scale with a high energy resolution detector facing to it. By scanning the sample's surface across the beam and acquiring the XRF spectra on each point and integrating their intensities in a defined window of energies the elemental map on the sample is obtained.

EXAFS/XANES, oxidation state mapping. The μ-EXAFS/XANES provides both structural and chemical information on specific targeted elements. Combined with mapping capabilities an array of μ-XANES measurements can be performed on a defined ROI allowing obtaining the 2D distribution of the oxidation state of an element. Depending on the sample, the experimental layout can be both in transmission for highly concentrated and thin samples or fluorescence for diluted and thick samples. In transmission geometry two ion chambers placed one in front and a second one behind the sample are used to measure the absorption edge during an energy scan. However in fluorescence geometry only one ion chamber is used and a high resolution fluorescence detector is placed instead. For selected elements μ-EXAFS/XANES normalization and fitting would allow us to determine their local environments.

XRD mapping to identify crystalline phases. The μ-XRD is one of the most popular techniques amongst Spanish scientists. It allows obtaining single diffraction patterns on selected points at micron scale but when combined with mapping capabilities an array of measurements can be performed on a defined ROI allowing obtaining the 2D distribution of the crystalline phases. The experimental layout in this type of measurements is based in transmission geometry with a sample cross section sitting between the end of the focusing optics and a CCD detector that records the powder diffraction rings. The diffraction pattern is obtained by integrating these rings and afterwards is used for phase identification by measuring the intensities and positions of the diffraction peaks.

SAXS/WAXS mapping, to detect long range order in the nm scale. This technique is a natural extension of the capabilities of the beamline, as it would use the same setup and detector as the XRD. With a small sub-micrometer beam, SAXS/WAXS diagrams can be obtained by just adding a small and precise beam stopper, which allows to use the CCD camera at a relatively short distance from the sample.

Beamline components

Taking into account the present needs of the Spanish users as well as those envisaged for the future, the basic technical requirements of a microfocus beamline in a medium energy source would be the following.

Source

An undulator source is the best solution to fulfill the principal requirements such as high spectral brightness, full energy, tunability with tapering capabilities in the 2-20 keV energy range. The most adapted insertion device to obtain a continuous energy spectrum without significant intensity gaps is an in-vacuum cryo-cooled undulator. In order cover the range of energies between 2 and 20 keV without gaps, one needs short period, and high field. In this sense, the hybrid magnet technology is the one that provides highest field for small periods.

Figure 24 shows the tuning curves for flux for a hybrid in vacuum undulator with the characteristics given in Table I. One can see that it provides flux around 10^{14} ph/s/0.1%BW for the whole energy range of the beamline, using up to the 11th harmonic.

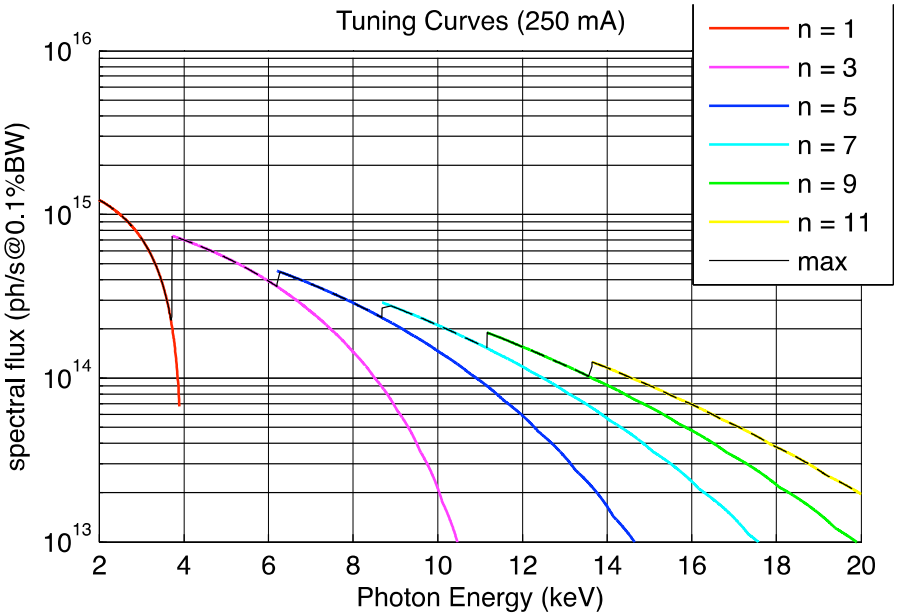

Figure 24: Tuning curves for the proposed in-vacuum undulator.

Table I: Parameters of the proposed undulator

Parameter	**Value**
Period	21.5 mm
Length	2.0 m
Max. K_y	2.15
Min Gap	4.8 mm

A low-beta straight section will offer the best flexibility by tuning the photon flux/spatial resolution ratio matching various experimental requirements. Special attention should be paid to the low emittance of the source but also its long and short-term stability as well as angular emissions to avoid frequent realignments of the beamline instrumentation. Almost all operational or under construction microprobe beamlines worldwide are built on an undulator source.

For the considered photon energy range, the horizontal size and divergence are given by the electron beam size. In the vertical direction, however, there is a significant contribution of the diffraction limit of the source, which depends on the photon energy. The root mean square values for the vertical source size and divergence are given in Figure 25.

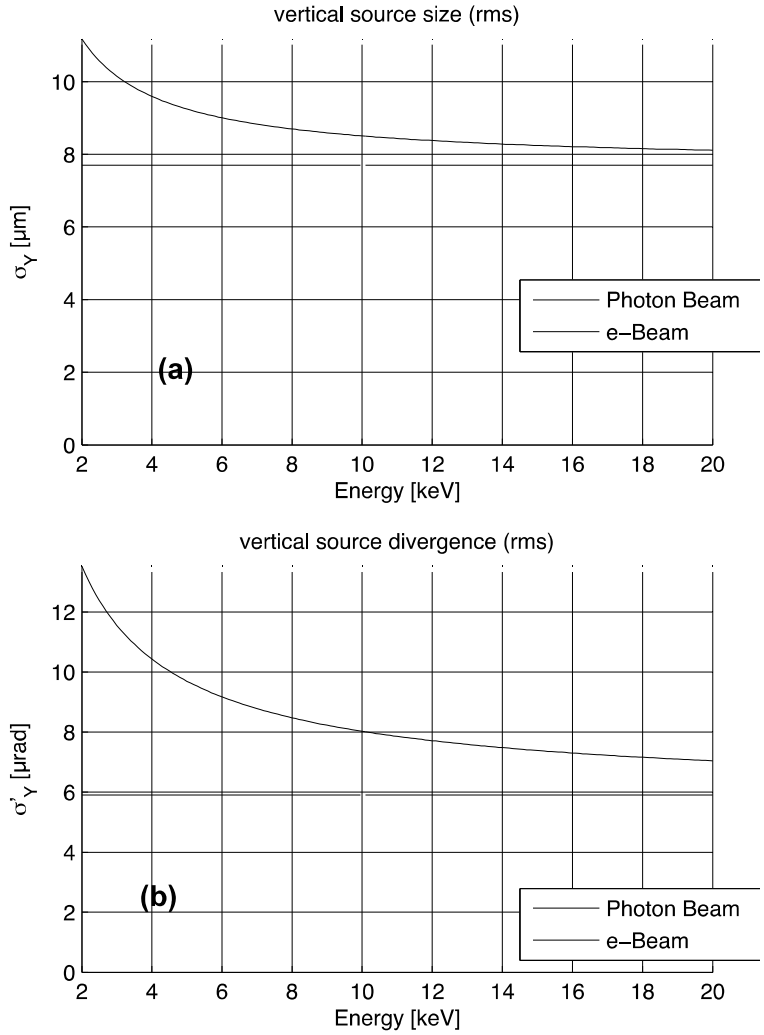

Figure 25: Vertical source size (a) and divergence (b) of the proposed undulator in a medium straight section of ALBA

Beamline optics

Since the photon source is small enough in the vertical direction, a single demagnification stage is enough in the vertical plane. On the other hand, two demagnification stages are required to achieve the required spot size in the horizontal direction. The corresponding layout proposed for the beamline is given schematically in Figure 26. Besides the front-end apertures and other diagnostic units, the monochromator is the first optical element of the beamline. It receives directly the radiation emitted by the undulator. Downstream the monochromator, i.e. already in the monochromatic section, a horizontally deflecting plano-elliptic mirror (HFM1) refocuses the source horizontally on a set of slits (S1). In addition, at fix 2.5 mrad nominal incidence angle, Si and Rh coatings on HFM1 will ensure efficient higher harmonics rejection in the full energy range. The working aperture for these slits is

around 25 µm. The slits define the horizontal source for the second demagnification stage of the beamline. At the very end of the beamline, close to the sample position there is a pair of plano-elliptic mirrors in Kirkpatrick-Baez configuration. The upstream mirror is the vertically focusing mirror (VFM) which focuses the source directly on the sample. The downstream mirror (HFM2), just 400 mm upstream the sample, focuses the slits onto the sample.

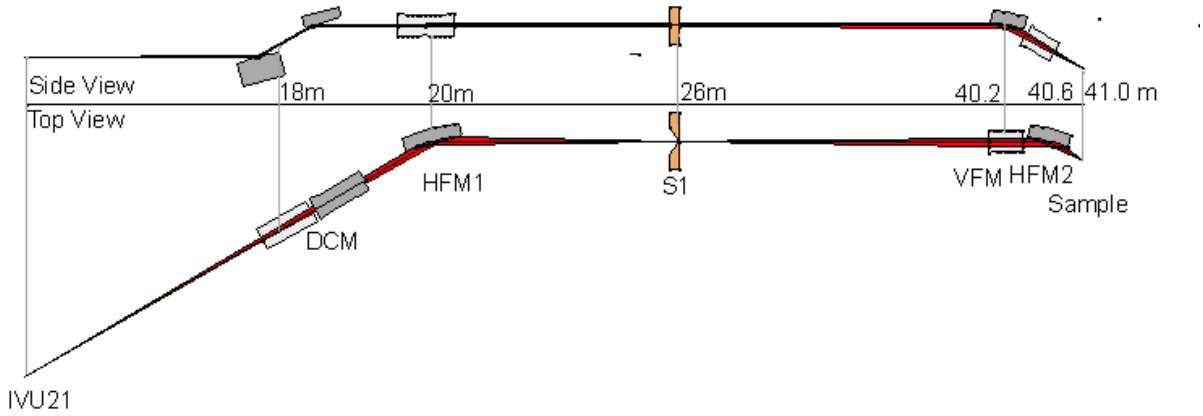

Figure 26: Proposed optical layout of the microfocus beamline

A ray-tracing calculation of the spot corresponding to the proposed layout is given in Figure 27. There we have assumed slope errors of 80 nrad rms, specification which is already achieved by two similar mirrors at ALBA, and which is also accepted by some suppliers.

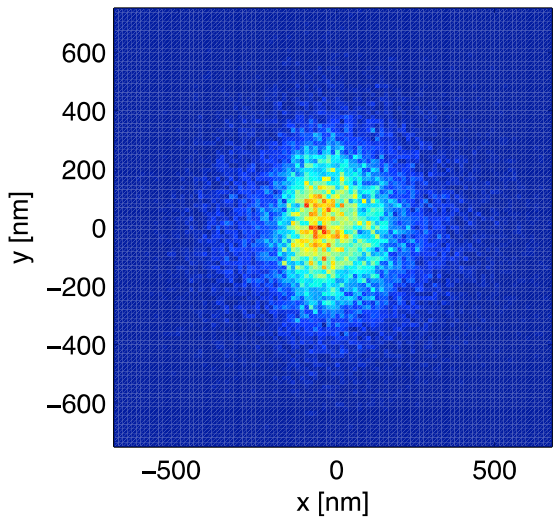

Figure 27: Spot on sample, at 10 keV

Monochromator

Given the low photon energy that the beamline will reach, the monochromator needs to work at very high Bragg angles on Si(111). Because of this, we propose a double crystal monochromator (DCM), as it can preserve the height offset of the beam with reasonable size optics a double crystal monochromator.

Another advantage of the DCM is that it can allocate space for a more than one pair of crystals. Different pairs of crystals with variable spacing should be available. The monochromator design must allow simple and quick changes of the crystal pairs in use, offering the user community several choices depending upon their requirements for X-ray flux and energy resolution in the operational energy range. For instance, Si (111) and Si (511) crystals could cover from 2 keV up to 20 keV operation, with intrinsic energy resolutions ranging from approximately 1 x 10^{-4} for the Si (111) to 1 x 10^{-5} for the Si (511). This is well inside the core hole lifetime broadening of the absorption edges within their operational energy ranges. Its mechanical stability and fixed-exit capabilities should be particularly optimized to keep the microbeam very stable during XAS acquisitions. Prrecise cooling schemes must be carefully analyzed to minimize vibrational and angular instabilities causing short and long term drifts.

This system would also allow a special set of multilayer mirrors, having a low energy resolution, high flux option for the beamline in the case of XRD measurements. This would be an alternative to the multilayer stripe in the refocusing Kirkpatrick-Baez system (as explained below), which could do the monochromator function. This alternative would imply that the white beam would not need to reach the experimental hutch directly, that would force us to have cooling in all the optical elements, and increase the radiation shielding in the experimental hutch.

Focusing system

For the final focusing of the beam onto the sample, we believe a Kirkpatrick-Baez (KB) mirror system would be the best choice. Although its alignment is more difficult than in the case of an inline focusing device (e.g., diffractive Fresnel zone plates and refractive microoptics-CRL), being based on total external reflection presents intrinsic advantages: high achromaticity (position and shape of the microbeam do not depend on the energy), excellent efficiency (large numerical aperture and high reflectivity), high spatial resolutions and long working distances. Thus, compared to other X-ray lenses, the KB system would ensure high flux and the possibility of easy energy tuning without realignment of the set-up, key requirements for XAS technique. We would propose a multi-striped KB system with Rh and/or Ir and Si stripes.

When only a monochromatic beam is needed (in XRD, SAXS/WAXS experiments), we propose a multilayer coating instead of a total-reflection one on the KB mirrors. In this scheme, the monochromator would be moved away from the beam, letting the white beam reach the HFM1, that would deliver the beam onto the KB system. Then, the multilayer would act as a low energy resolution monochromator and focusing device at the same time. By removing two of the optical components, we would get a strong increase on the X-ray flux at the sample, at the cost of lower energy resolution. This would be interesting for experiments that do not need a high monochromaticity of the incoming X-ray, but are photon-hungry (like some imaging applications).

In summary, we propose to combine different stripes on the KB mirrors. One stripe would be a multilayer coating, and the others would be total-reflection coatings Rh and/or Ir and Si. For spectroscopy experiments, single coating stripes would be used, at grazing incidence of 4 mrad, while for high-flux diffraction experiments the multilayer coating would be used. Figure 28 shows the reflectivity for the proposed Ir and Rh coatings in the considered energy range of the beamline.

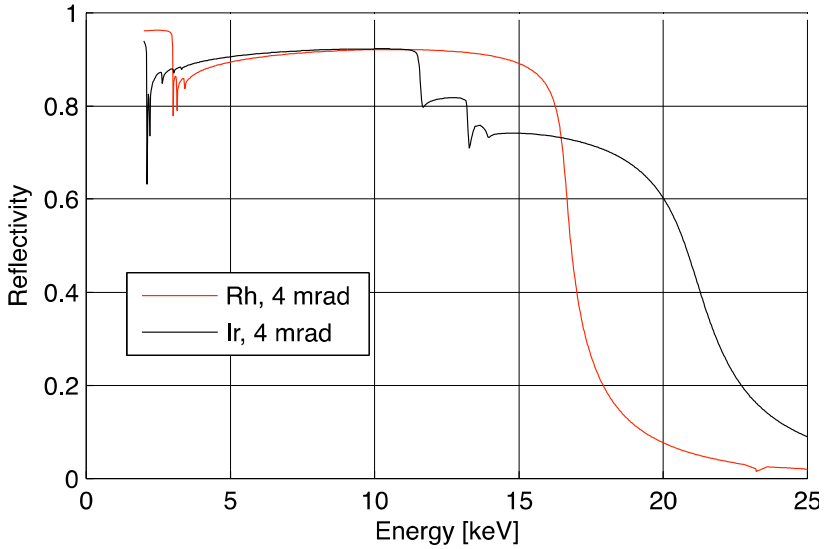

Figure 28: Reflectivity of the single coating mirrors

The most important requirements for the KB elements are its high optical quality (small roughness and slope error). Also, its sensitivity to angular variations of the incident beam could play a key role. The high stability of the electron beam at ALBA as well as the top-up filling mode could result in constant heat-load at the main optical elements, being especially advantageous to minimize the angular instability of the X-ray beam.

Another aspect we have taken into account is the strong variation of the incidence angle along the mirror length, which is a consequence of the variation of the radius of curvature, which at the same time, depends on the demagnification of the optics. A consequence of this is the fact that, at the downstream end of the mirror, the local incidence angle may be above the critical angle, what is a de-facto limit of the mirror acceptance for total reflection coatings. In the case of the multilayer coatings, the gradient of the layer period is designed to compensate for this limitation in mirror length. Nevertheless, this is optimized for only one photon energy, and yields to a decrease of the mirror acceptance for other energies.

Another factor limiting the utile length of the mirror is given by the ellipse approximation of the bender. Although the mirror width can be profiled to obtain the ideal ellipse for a given incidence angles, only the defocusing and spherical aberration can be controlled for different incidence angles. This means that, to preserve the aberrations below a certain level (equivalent to a slope deviation of 100 nrad rms) one needs to limit the area of the mirror that is illuminated, as a function of the incidence angle. This is illustrated in Figure 29, where it is shown the utile mirror length for HFM2 as a function of the incidence angle.

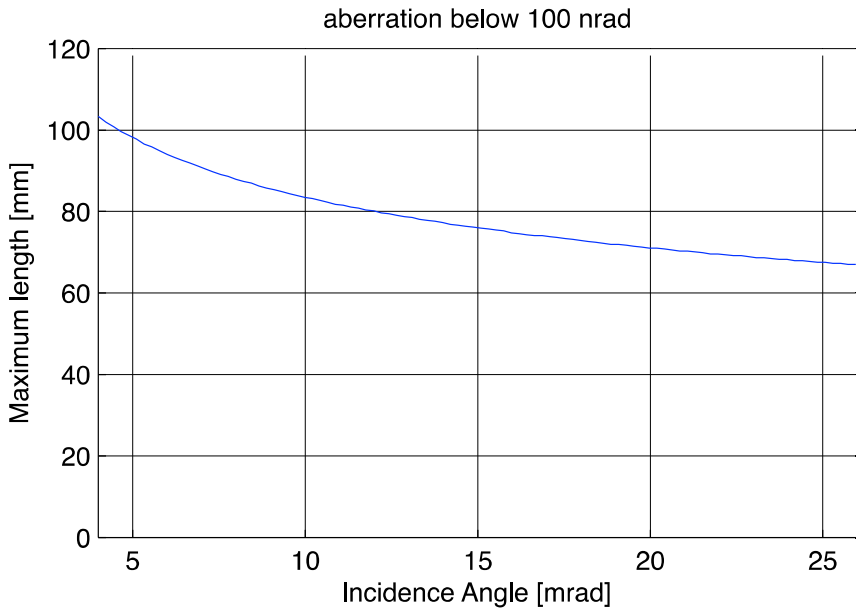

Figure 29: Utile length of the HFM2 mirror, as a function of the incidence angle

Layout optimization

In order to optimize the layout, the possible positions of the first demagnification stage have been explored using an analytical model of the spot size and the flux density on sample. The model considers the following contributions to the spot size and the mirror footprint: source size, source divergence, diffraction limit of the mirrors, slope errors of the mirrors, slit size, diffraction at the slit, and aberrations of the bender (assuming linear variation of the mirror width).

The spot size on sample, as well as the flux on the spot are computed for the different positions of the HFM1, and of the slit S1. The result is shown in Figure 30. M1 represent the distance of HFM1 to the source, while qM1 is the distance from the mirror to the slits. The figure shows the flux on sample for those configurations that provide a spot below 0.5 μm. The choosen values M1=20 m and qM1=6m corresponding to a configuration that can confortably reach the specification, which is compatible with the ALBA layout, and that provides a high acceptance of the source.

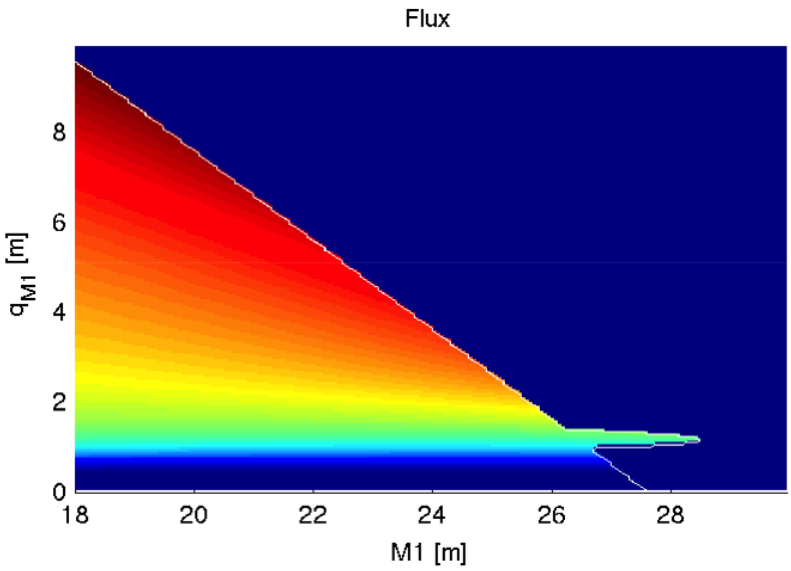

Figure 30: Map of possible configurations for the first demagnification stage. The flux on sample, for configurations that reach 0.5 μm spot size are represented

Stability considerations

One of the aspects that have to be considered for the beamline is how robust it is to fluctuations of the source and or the optical components. In this sense, the usage of the horizontal slits S1, which are overfilled, isolates the spot on sample from horizontal fluctuations of the source, the monochromator or HFM1. In addition the slits are already at the monochromatic section of the beamline, and do not require cooling, which is a potential source of vibrations.

Regarding the vertical direction, the main source of oscillations will be the monochromator, To minimize the impact of its vibrations it has been placed as close to the source as possible (still in the experimental hall). Additionally one could consider having a horizontal dispersion monochromator, in which case the vibrations would be isolated by the slits. The main drawback for that configuration, in any case, would be the poor transmission of the p-polarization component at the monochromator, for low photon energies.

Experimental station

The beamline will be optimized for medium and hard X-ray microanalysis detectors in a broad energy range from 2 to 20keV consisting in the combination of X-ray fluorescence, X-ray absorption spectroscopy and X-ray diffraction, with 2D and 3D imaging techniques in a second-stage. The instrument will be available and applied to medicine, biology, earth and planetary sciences, environmental science, archaeometry and materials science. Thus, keeping the basic principles of these research fields with high adaptability a modular approach could be foreseen to accommodate various configurations and combination of different techniques. These disciplines seek for non-destructive investigation of the spatial distribution, concentration and speciation of trace elements to be correlated to the morphology and crystallographic orientations at the micrometer levels.

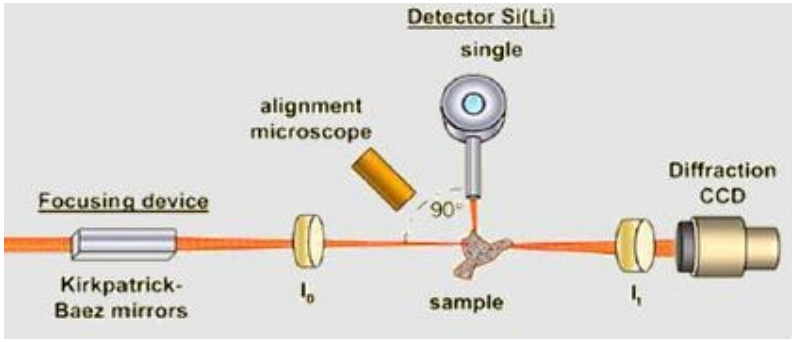

Figure 31: Scheme of the sample environment, highlighting the multidetector setup

In principle, the microprobe setup could be located on a very stable and moveable table ensuring multiple beam operation modes (white, pink, monochromatic, monochromatic + reflected). Anticipating horizontal and vertical translations, they will allow the expansion of the scientific activities to novel applications in long-term (e.g., tomographic techniques).

The sample stage must be robust and versatile, designed and optimized for different acquisitions and sample environments, allowing not only the accommodation of common sample holders like goniometer heads, but also in-situ conditions such as high pressure cells, micro-furnace, mini-cryostats, etc. The long working distances and high penetration powers will allow the adaptation and development of various controlled sample environments. A XYZ piezo-scanner could be also coupled to guarantee high precision and excellent resolutions scanning capabilities. In addition, to improve the detection efficiency of low Z elements, reducing the scattering contribution from air, and to ensure the access to absorption edges at lower energies, a vacuum or He chamber must also be designed.

For X-ray fluorescence acquisitions, the installation of a large solid angle multielement detector, with a concentric and oriented array, could give tremendous benefits in the scanning acquisitions. Also its complementary technology, compact silicon drift detectors which enable higher detection limits and counting rates at the expense of a slightly decreased energy resolution. To avoid strong spectral overlapping with the Si escape peaks at low energies, high purity Ge detector technology could be chosen for low energies. For fast readout, low noise and high efficiency in XRD and SAXS/WAXS acquisitions, a 2D detector (possibly a fast CCD camera) must be purchased, with suitable beamstoppers, mounted onto an horizontal moveable stage. For I_0 monitoring optimized gas-filled ionization chambers or the implementation of a photodiode coupled to a crossed scattering foil could be established, delivering a better signal-to-noise ratio than the standard setups.

In a second-stage, the design and implementation of the retractable tomography stage upstream from the focusing optics would be a priority, guarantying not only complementary imaging information with high precision and repeatability, but also an easy and quick switch with the focusing optics in use.

Concerning offline facilities, computing power, large data storage capabilities and network speed will be issues given the large data sets that will be obtained and analyzed.

Cost estimation

The budget estimate for the entire beamline is summarized in Table II based on ESRF technical services.

The first optics hutch should be compatible with white beam radiation. The two main beamline optics are the white beam mirror and the fixed-exit double crystal monochromator. Their price could exceed the standard estimates because extreme stability is necessary, local metrology is included and/or fast energy scanning is required (XAS monochromator). Some major items in terms of cost can be phased in time. The development of a robust fixed-exit monochromator for XAS applications is a top priority for the success of the microprobe and must be conducted in close collaboration with an external company.

Table II: Cost estimation of the proposed beamline

Major Item	k€	Comment
Undulator+frontend	950	Hybrid magnet in-vaucuum undulator
Lead optical hutch	300	Dimensions: 10 m long, 2.5 m wide, 3.4 m high
OH services	250	Control cabines cabling, electricity, fluids
Lead experim. hutch	250	Dimensions: 10 m long, 4.5 m wide, 4 m high
EH services	600	Cabling, air conditioning, electricity, fluids
Instruments hutches	400	Shutters, collimators, BPMs, filters, slits, cryocooler,
Tubes and shielding	250	Transport of pink beam
Vacuum equipment	200	Vacuum pumps and gauges
White beam mirror	350	High quality cooled and coated crystal + motorization
Double crystal monochromators	900	Fast scanning and coherence preservation
Table	60	Granite support and motorization
Focusing optics	250	High quality KB mirrors system
Sample stage	120	XYZ, encoders, piezo-scanner
Detectors	600	Energy dispersive detectors and area detector
Control electronics	300	Motors and general control electronics
Support laboratory	60	Visible light microscope for sample alignment
Network	60	Plugs, 10 Gbe clients
Subtotal	5900	
Contingencies	590	10% of subtotal
Total estimate	6490	

Future development

Although it is premature to set precise future developments, some of the most desirable instrumentation plans after the beamline become operational are:

1. The diffraction capabilities could be easily expanded to other diffraction based modes like projection X-ray micro-diffraction, resonant X-ray diffraction holography imaging, and X-ray ptychography imaging.

2. Access to μ-XRF tomography. This technique would provide with 3D compositional maps of the samples. It would require a precise rotating sample stage and dedicated software for imaging reconstruction.

3. An additional important development could be the confocal XRF detection using a polycapillary half-lens, acting as a spatial filter for micro-XRF applications where background radiation from areas not in the region of interest interferes with the signal of interest. Therefore the detection sensitivity and accuracy is greatly improved. Another possible application of the confocal geometry is depth profiling, acting as a layered material probe by detecting emitted XRF only from the intersection of the output focal spot of the excitation optic and the input focal spot of the collection optic. As a result, it is an excellent tool to study buried structures by depth-sensitive X-ray absorption spectroscopy in fluorescence detection mode at the micrometer scale.

4. To cover a number of life-sciences experiments under their native states, and to address problems with complementary techniques that to those of MISTRAL, the implementation of a cryo stage capable of with a cryo transfer load-lock system could be anticipated.

5. Explore the potential of Compton-scattered photons to obtain electron density maps - including software developments for data taking strategy and visualization.

6. Design innovative detection configurations and collimation technologies to maximize the detection efficiency for both energy dispersive detectors for XRF and 2D detectors for imaging.

7. Develop an ancillary laboratory with micro-analytical and micro-manipulation tools in the neighboring of the beamline.

8. Develop data analysis strategies - multi-spectral imaging will require new statistical data processing as already developed in other microscopy methods.

9. Implement retractable systems for essential components like sample manipulators, optical microscopes, etc.

10. Explore new capabilities like linear dichroism microscopy and wavelength dispersive X-ray spectroscopy.

Links to Horizon 2020 programme

Horizon 2020 is the biggest European Union research and innovation programme, that acts as the financial instrument to ensure that Europe produces world-class science and technological innovation, with the maximum impact on society.

It comprises three major sections: Excellent Science, Industrial Leadership and Societal Challenges. Each of them es divided in subsections that contain different calls for research and innovation projects related to the fields considered to be a priority for European industry and society.

Being an intrinsically multidisciplinary beamline, the scientific case of this proposal fits in several of these calls, some of which are listed here.

Excellent Science

4. European research infrastructures (including e-Infrastructures)

INFRAIA-1-2014/2015: Integrating and opening existing national and regional research infrastructures of European interest

This call promotes the construction of research infrastructures with the following fields in mind, among others:

- *Environmental and Earth Sciences*
  - Research infrastructures for research on crustal fluids and geo-resources
- *Social Sciences and Humanities*
  - European research infrastructures for restoration and conservation of cultural heritage
- *Engineering, Material Sciences, and Analytical facilities*
  - Advanced nanofabrication
  - Advanced frontier research in nanoelectronics
  - Facilities for research on materials under extreme conditions
- *Biological and Medical Sciences*
  - Research Infrastructures for translating research on biological structures into
  - innovation in biomedicine (such as X-ray and neutron scattering (…))

Industrial Leadership

5. Leadership in enabling and industrial technologies

i. Information and Communication Technologies

ICT 3 – 2014: Advanced Thin, Organic and Large Area Electronics (TOLAE) technologies

This call proposes to advance in the research of new materials for micro and

nanoelectronics, including semiconductors, organic materials, thin films among others. We can quote that the objectives are *«...to advance the state of the art of TOLAE technologies and manufacturing processes and increase the performance, functionality and complexity of TOLAE devices suitable for smart systems»*. This is in direct relation with some of the scientific examples presented above, specially in the Hard and Soft Condensed Matter sections.

Societal Challenges

8. Health, demographic change and wellbeing

PHC 1 – 2014: Understanding health, ageing and disease: determinants, risk factors and pathways

This is one of the health-related calls that fits better with one of the bio-medical applications presented above. It aims to *«...the identification of health trends and determinants, their validation, and the validation of risk factors for disease and disability, through the generation, integration and validation of data derived from relevant disciplines (e.g. molecular, behavioural, nutritional, clinical, social and environmental epidemiology; exposure sciences; genetics, epigenetics, etc.)»*.

12. Climate action, environment, resource efficiency and raw materials

SC5-8-2014: Preparing and promoting innovation procurement for soil decontamination

This action states that *«Soil contamination is typically caused by industrial activity, mining and smelting practices, agricultural chemicals or improper disposal of waste and is increasingly becoming a very serious environmental and health problem (...) It is therefore crucial for public authorities to be able to identify the most fit-for-purpose and cost-effective solutions»* The proposed beamline would be able to study the characteristics of various kinds of soil contamination, which would lead to find the best solutions.

13. Europe in a changing world – inclusive, innovative and reflective Societies

Call - Reflective Societies: Cultural Heritage and European Identities

This call aims, among other things, to use the most advanced technologies to aid the study and conservation of the European cultural heritage. For instance *«This call (...) will also foster the potential of digital technologies for facilitating the modelling, analysis, understanding and preservation of European cultural heritage (...)».* Techniques like XRF mapping or X-ray imaging specifically intend to fulfill this issue.

Institutional support

A few research centers and institutions in Spain have expressed their explicit support on the construction of the beamline proposed in this project. Herein we reproduce the support letters received.

MINISTERIO
DE ECONOMÍA
Y COMPETITIVIDAD

CSIC
CONSEJO SUPERIOR DE INVESTIGACIONES CIENTÍFICAS

ASUNTO: Apoyo a propuesta a la propuesta de desarrollo de una línea microfocal de fluorescencia, difracción y absorción de rayos X en la nueva fase (II) de construcción del Sincrotrón ALBA-CELLS.

Madrid, 1 de abril de 2014

Estimado Dr. Fernando Garrido,

Como Coordinador del Área Científica de Recursos Naturales del Consejo Superior de Investigaciones Científicas quiero expresar nuestro apoyo a la propuesta de desarrollo de una línea microfocal de fluorescencia, difracción y absorción de rayos X en la nueva fase (II) de construcción del Sincrotrón ALBA-CELLS.

El empleo de técnicas analíticas basadas en la radiación sincrotrón en proyectos y estudios de Ciencias Ambientales y de la Tierra es uno de los avances científicos y tecnológicos más significativos de los últimos años. Un número creciente de investigadores acuden a estas técnicas para avanzar en el conocimiento de procesos y fenómenos de la naturaleza a escala molecular. El acceso a líneas de radiación sincrotrón con resolución micro y nanométrica permite superar las dificultades derivadas de la heterogeneidad y complejidad propias de los materiales objeto de estudio en el ámbito de los Recursos Naturales. Por tal motivo, la construcción de una línea microfocal en la nueva fase de desarrollo del sincrotrón ALBA es esencial para el avance en nuevos proyectos de muchos de los grupos de I+D del área que coordino, fortaleciendo además a los grupos nacionales en la obtención competitiva de fondos en convocatorias nacionales y europeas.

Sin otro particular,

Dr. Xavier Querol

SOCIEDAD ESPAÑOLA DE MINERALOGÍA
Museo Nacional de Ciencias Naturales
C/ José Gutiérrez Abascal 2
28006 Madrid

Barcelona, 2 de abril de 2014

Estimado Dr. Fernando Garrido,

Como Presidente de la Sociedad Española de Mineralogía (SEM) quiero expresar nuestro apoyo a la propuesta de desarrollo de una línea microfocal de fluorescencia, difracción y absorción de rayos X en la nueva fase (II) de construcción del Sincrotrón ALBA-CELLS.

Un número creciente de investigadores socios de la SEM aprovechan el potencial científico de las técnicas de espectroscopía de absorción de rayos X basadas en la radiación sincrotrón. Sin embargo, el acceso a líneas con resolución micro y nanométrica permite superar las dificultades derivadas de la heterogeneidad y complejidad propias de los materiales geológicos objeto de estudio en el ámbito de la Mineralogía, Petrología y Geoquímica. Por tal motivo, la construcción de una línea microfocal en la nueva fase de desarrollo del sincrotrón ALBA supondría un gran apoyo en la investigación desarrollada por los asociados de la SEM a los que represento, fortaleciendo además a nuestros grupos para la obtención de fondos en convocatorias competitivas nacionales y europeas.

Estoy a tu disposición para aportar detalles si lo crees necesario,

Carlos Ayora

SECS
Sociedad Española
de la Ciencia del Suelo

ASUNTO: Apoyo a la propuesta de desarrollo de una línea microfocal de fluorescencia, difracción y absorción de rayos X en la nueva fase (II) de construcción del Sincrotrón ALBA-CELLS.

Madrid, 3 de abril de 2014

Estimado Dr. Fernando Garrido

Dado que las técnicas de espectroscopía de absorción de rayos X basadas en la radiación sincrotrón están permitiendo avanzar en el conocimiento de muchos de los procesos (bio)geoquímicos que se producen en el suelo, un número creciente de investigadores de la SECS aprovecha su potencial científico en proyectos relacionados con la biología, química y mineralogía del suelo tanto en el ámbito de la conservación y protección del suelo, en estudios de los procesos involucrados en su contaminación y regeneración o incluso en múltiples aspectos relacionados con la productividad del suelo. El acceso a líneas con resolución micro y nanométrica permitiría superar las dificultades derivadas de la heterogeneidad y complejidad propias de los materiales edáficos. La construcción de una línea microfocal en la nueva fase de desarrollo del sincrotrón ALBA supondría un gran apoyo en la investigación desarrollada por los asociados de la SECS a los que represento, fortaleciendo además a nuestros grupos para la obtención de fondos en convocatorias competitivas nacionales y europeas.

Por todo ello, como Presidente de la Sociedad Española de la Ciencia del Suelo (SECS) **quiero expresarle nuestro apoyo** a la propuesta de desarrollo de una línea microfocal de fluorescencia, difracción y absorción de rayos X en la nueva fase (II) de construcción del Sincrotrón ALBA-CELLS.

Muy cordialmente,

Dr. Jaume Porta

Table of users

The following is a compendium of users that have either expressed support on the construction of the beamline proposed, and/or have already performed experiments in a similar beamline, sometimes with published results.

Name	Address	e-mail	Field	Techniques	Energy ranges	Límit concentr.	Spatial resolution	Experience/ publications
PELLICER PORRES, Julio	Departamento de Física Aplicada-ICMUV, MALTA Consolider Team, Universitat de València, 46100 Burjassot (Valencia), Spain	Julio.Pellicer@uv.es	Materials	XAS, XRD, XRF, high pressure	Hard X-rays	-	1x1 μm^2	Y/Y
MARTINEZ-CIRADO, Gema	European Synchrotron Radiation Facility, 38043 Grenoble Cedex, France.	gmartine@esrf.fr	Materials	XAS, XRD, XRF, XRI	Hard X-rays	-	-	Y/Y
SANS TRESSERRAS, Juan Angel	Universidad Politécnica de Valencia, Cno. de Vera, s/n. 46022 Valencia	juasant2@upv.es	Materials	XAS, XRD, XRF, high pressure	Hard X-rays	1 ppm	1x1 μm^2	Y/Y
LAVÍN DELLA VENTURA Víctor	Departamento de Física. Universidad de La Laguna. 38200 San Cristóbal de La Laguna, Santa Cruz de Tenerife,	vlavin@ull.edu.es	Materials	XAS, XRF, XRD, high pressure	1-35keV	0.001 – 0.01 mol%	100 nm^2	Y/Y
TOBIAS Gerard	Institut de Ciencia de Materials de Barcelona (ICMAB-CSIC) Campus UAB 08193 Bellaterra (Barcelona),	gerard.tobias@icmab.es	Materials	-	-	-	-	N/N
VALIENTE Rafael	Dpto. Física Aplicada, Fac. Ciencias, Universidad de Cantabria; Avda. de Los Castros s/n, 39005 Santander	rafael.valiente@unican.es	Materials	XAS, XRD, XRF, high pressure	Hard X-rays	1 ppm	1x1 μm^2	Y/Y
HERNÁNDEZ MÁRQUEZ, Sergio	Departamento de Electrónica, Facultad de Física, Universidad de Barcelona	shernandez@el.ub.es	Materials	XRD, XRF	5-50 keV	10-100 ppm	500nm-1 µm	

Name	Address	e-mail	Field	Techniques	Energy ranges	Límit concentr.	Spatial resolution	Experience/ publications
LLORCA Jordi	Institute of Energy Technologies Technical University of Catalonia - BarcelonaTECH	jordi.llorca@upc.edu	Materials					
FERNANDEZ-GUBIEDA M. Luisa	Departamento de Electricidad, Facultad de Ciencia y Tecnología, Universidad del País Vasco	malu@we.lc.ehu.es	Materials	XAS, XRF, XRD				
LÓPEZ-FLORES, Víctor	Synchrotron SOLEIL, L'Orme des Merisiers, St-Aubin, B.P. 48, 91192, Gif-sur-Yvette, France	victor.lopez-flores@synchrotron-soleil.fr	Materials	XAS, XRI				
MUÑOZ-PÁEZ, Adela	Departamento de Química Inorganica, Universidad de Sevilla, Instituto de Ciencia de Materiales de Sevilla, CSIC	adela@us.es	Materials, Cultural heritage	XAS, XRF, XRD				Y/Y
ODRIOZOLA GORDON, José Antonio	Departamento de Química Inorganica, Universidad de Sevilla, Instituto de Ciencia de Materiales de Sevilla, CSIC	odrio@us.es	Materials	XAS, XRF, XRD	5-30 keV			
BIKONDOA Oier	XMaS-BM28 (ESRF) para la Univ. of Warwick (www.xmas.ac.uk)	oier.bikondoa@esrf.fr	Materials	XRD, XRF			<100 nm^2	Y/Y
FERNÁNDEZ-GARCÍA Marcos	ICP-CSIC	mfg@icp.csic.es	Materials	XAS, XRD, XRF, time resolution	2-30 keV			
EZQUERRA Tiberio	Grupo de Materia Condensada Blanda y Polimérica, Instituto de Estructura de la Materia, CSIC. Serrano 121, 28006-Madrid	t.ezquerra@csic.es	Materials (Soft)	XRD, SAXS, WAXS	2-20 keV	-	100 nm^2	Y/Y
GOMEZ-FATOU Marián	Departamento de Física de Polímeros. Instituto de Ciencia y Tecnología de Polímeros, CSIC. Juan de la Cierva 3, 28006-Madrid.	magomez@ictp.csic.es	Materials (Soft)	XRD, SAXS, WAXS	2-20 keV	-	100 nm^2	Y/Y
PÉREZ TABERNERO Ernesto	Grupo de Sistemas Poliméricos Nanoestructurados Instituto de Ciencia y Tecnología de Polímeros, ICTP-CSIC, Juan de la Cierva 3, 28006-	ernestop@ictp.csic.es	Materials (Soft)	XRD, SAXS, WAXS	8-13 keV	-	<1 μm^2	N/N

Name	Address	e-mail	Field	Techniques	Energy ranges	Límit concentr.	Spatial resolution	Experience/ publications
	Madrid							
HERNANDEZ RUEDA Jaime J.	Institut de Sciences des Matériaux de Mulhouse, CNRS UMR7361, CNRS, 15 rue Jean Starcky, Mulhouse 68057, France.	jaime.h@iem.cfmac.csic.es	Materials (Soft)	XRD, SAXS, WAXS	2-20 keV	-	100 nm^2	Y/Y
SANTORO Gonzalo	Beamline P03, PETRA III Forschung mit Photonen Deutsches Elektronen Synchrotron (DESY) Notkestr. 85, 22607 Hamburg, Germany.	gonzalo.santoro@desy.de	Materials (Soft)	XRD, SAXS, WAXS	5-20keV	-	200 nm^2	Y/Y
GÓMEZ, Marian	Department of Polymer Physics and Engineering. Instituto de Ciencia y Tecnología de Polímeros, CSIC. Juan de la Cierva 3, 28006-Madrid	magomez@ictp.csic.es	Materials (Soft)	XRD, SAXS, WAXS	5-20keV	-	200 nm^2	Y/Y
ELLIS, Gary	Department of Polymer Physics and Engineering. Instituto de Ciencia y Tecnología de Polímeros, CSIC. Juan de la Cierva 3, 28006-Madrid	gary@ictp.csic.es	Materials (Soft)	XRD, SAXS, WAXS	5-20keV	-	200 nm^2	Y/Y
REBOLLAR Esther	Lasers, nanostructures and materials processing Group. Instituto de Química Física Rocasolano, IQFR-CSIC, Serrano 119, 28006 Madrid.	e.rebollar@iqfr.csic.es	Materials (Soft)	XRD, SAXS, WAXS	2-20 keV	-	100 nm^2	N/N
RODRÍGUEZ PEREZ Miguel Angel	Cellular Materials Laboratory (CellMat), Departamento de Física de la Materia Condensada, Universidad de Valladolid, Paseo de Belén 7, 47011, Valladolid.	marrod@fmc.uva.es	Materials (Soft)	XRD, SAXS, WAXS	2-20 keV	-	200 nm^2	N/N
PUIGGALÍ BELLALTA, Jordi	Departamento de Ingeniería Química. Universidad Politécnica de Cataluña.	Jordi.Puiggali@upc.edu	Materials (Soft)	XRD, SAXS, WAXS	2-20 keV	-	200 nm^2	N/N
DENCHEV, Zlatan	Department of Polymer Engineering. University of Minho – Campus de Azurém. 4800-045 Guimarães,	denchev@dep.uminho.pt	Materials (Soft)	XRD, SAXS, WAXS	2-20 keV	-	200 nm^2	N/N

Name	Address	e-mail	Field	Techniques	Energy ranges	Límit concentr.	Spatial resolution	Experience/ publications
	Portugal							
GARCÍA-GUTIÉRREZ, Mari Cruz	Grupo SOFTMATPOL, Instituto de Estructura de la Materia, IEM-CSIC. Serrano 121, Madrid.	maricruz@iem.cfmac.csic.es	Materials (Soft)	XRD, SAXS, WAXS, XRF	2-20 keV	-	100 nm^2	Y/Y
CANTARERO Andrés	GES, University of Valencia	cantarer@uv.es	Materials	XRF, SAXS, WAXS	2-20 keV		100×100 nm^2	Y/Y
LOZANO-CASTELLO, Dolores	Dept. de Química Inorgánica. e Instituto Universitario de Materiales. Universidad de Alicante, Ap. 99, 03080 Alicante	d.lozano@ua.es	Materials, Environment	XRD, SAXS, WAXS	6-20 keV	-	100 nm^2	Y/Y
CAZORLA AMOROS Diego	Dept. de Química Inorgánica e Instituto Universitario de Materiales. niversidad de Alicante, Ap. 99, 03080 Alicante.	cazorla@ua.es	Materials, Environment	XRD, SAXS, WAXS	6-20 keV	-	100 nm^2	Y/Y
IBANEZ INSA Jordi	Instituto de Ciencias de la Tierra Jaume Almera (CSIC), c/ Lluís Solé i Sabarís s/n, 08028 Barcelona	jibanez@ictja.csic.es	Materials, Cultural heritage, Geochemistry, Earth science.	XRD y XRF	5-50 keV	10-100 ppm	500 nm-1 µm	N/N
ROLDÁN, Clodoaldo	Departamento de Fisica Aplicada C/ Dr. Moliner 50 46100 Burjassot (Valencia) Spain University of Valencia	clodoaldo.roldan@uv.es	Cultural heritage	XRD y XRF	-	Ppm/ppb	Eitherµm/ nm	N/N
PRADELL, Trinitat	Departament de Física i Enginyeria Nuclear Universitat Politecnica de Catalunya, BarcelonaTECH	Trinitat.Pradell@upc.edu	Cultural heritage	XAS, XRF y XRD	2-30 keV		1x1 μm^2	Y/Y
VALIENTE, Manuel	Departamento de Quimica, Universidad Autónoma de Barcelona	Manuel.Valiente@uab.es	Environment	XAS, XRF	2-20 keV			Y/Y
SABÉS XAMANÍ Manel	Universidad Autónoma de Barcelona Àrea de Bioquímica y Biologia Molecular	manel.sabes@uab.ca	Life Sciences, Biomedicine	XAS, XRF	2-20 keV		1x1 μm^2	Y/Y

Name	Address	e-mail	Field	Techniques	Energy ranges	Límit concentr.	Spatial resolution	Experience/ publications
GARCÍA VERDUGO José Manuel	Neurobiología Comparada, Universidad de Valencia	j.manuel.garcia@uv.es	Life Sciences, Biomedicine	XRF, XRD	2-12 keV		100×100 nm^2	N/N
POSCHENRIEDER, Charlotte	Lab. Fisiologia Vegetal Facultad Biocoencias Universidad Autónoma de Barcelona	Charlotte.poschenrieder@uab.es	Life Sciences, Environment	XRF	2-20 keV			Y/Y
GARRIDO, Fernando	Museo Nacional de Ciencias Naturales (MNCN-CSIC), 28006 Madrid	fernando.garrido@mncn.csic.es	Geochemstry, Earth sciences	XRF,XAS	2-20 keV			Y/Y
ÁLVAREZ-LLORET, Pedro	Dpto. MINERALOGIA y petrología, Fac. Cieoncias Univ. Granada	pedalv@ugr.es	Geochemstry, Earth sciences	XRF,XAS	2-20 keV			
SERRANO, Susana	Instituto de Agroquímica y Tecnología de Alimentos, 46980 Paterna (Valencia).	sserrano.parearroyo@gmail.com	Geochemstry, Earth sciences	XRF,XAS	2-20 keV			
YESARES, Lola	Departamento de Geología, Universidad de Huelva, 21071, Huelva	Lola.yesares@dgeo.uhu.es	Geochemstry, Earth sciences	XRF,XAS	2-20 keV			
PEREZ-LOPEZ, Rafael	Departamento de Geología, Universidad de Huelva, 21071, Huelva	rafael.perez@dgeo.uhu.es	Geochemstry, Earth sciences	XRF,XAS	2-20 keV			Y/Y
ASTA-ANDRES, María Pilar	Insituto Andaluz de Ciencias de la Tierra, Armilla, Granada	masta@iact.ugr-csic.es	Geochemstry, Earth sciences	XRF,XAS	2-20 keV			Y/N